TRANSLATION

AUTOMATIC WELDING
(SELECTED ARTICLES)

FOREIGN TECHNOLOGY DIVISION

AIR FORCE SYSTEMS COMMAND

WRIGHT-PATTERSON AIR FORCE BASE

OHIO

UNEDITED ROUGH DRAFT TRANSLATION

AUTOMATIC WELDING (SELECTED ARTICLES)

English Pages: 65

SOURCE: Russian Periodical, Avtomaticheskaya Svarka, Nr. 5, 1962, pp. 1-24, 57-63, 78-88

S/125-62-0-5

THIS TRANSLATION IS A RENDITION OF THE ORIGINAL FOREIGN TEXT WITHOUT ANY ANALYTICAL OR EDITORIAL COMMENT. STATEMENTS OR THEORIES ADVOCATED OR IMPLIED ARE THOSE OF THE SOURCE AND DO NOT NECESSARILY REFLECT THE POSITION OR OPINION OF THE FOREIGN TECHNOLOGY DIVISION.	PREPARED BY: TRANSLATION SERVICES BRANCH FOREIGN TECHNOLOGY DIVISION WP-AFB, OHIO.

TABLE OF CONTENTS

A DECATRON PROGRAMMING UNIT

B.Ye. Paton, V.S. Gavrish and Yu.S. Grodetskiy

(Order of the Red Banner of Labor Electric Welding Institute imeni Ye.O. Paton, Acad. Sci. UkrSSR)

A new programming unit with the program recorded on a fixed punch card has been developed. The time sweep is accomplished with decatrons.

A universal device for programming regimes of fast processes of resistance welding was described in [1]. Tests under laboratory and working conditions showed that the unit enables us to increase the quality of the welded joints and to expand the technological possibilities of resistance welding.

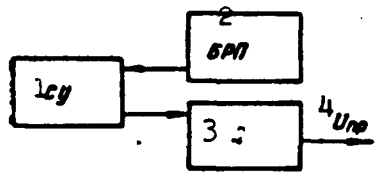

Fig. 1. Block diagram of programming unit. SU) Readout unit; BRP) program time-sweep unit; D) decoder. 1) SU; 2) BRP; 3) D; 4) U_{pr}.

While it has a series of advantages, the universal programming unit also has certain drawbacks: the necessity of using mechanical elements for the program input; the impossibility of quick program repetition after completion of the preceding cycle, since the program starts from a certain place on a perforated disk (the start-synchronization hole); comparatively large numbers of electron tubes and thyratrons. The above drawbacks are completely eliminated in a new, simpler and more reliable model.

Working principle of unit. The welding conditions (the duration

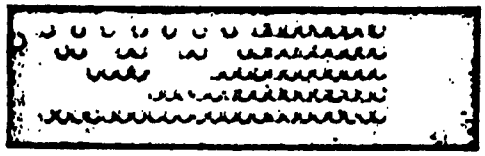

Fig. 2. Punch card.

of the welding-current pulse and the break and shape of the current curve) are assigned on the program carrier in binary code [1]. A block diagram of the programming unit is shown in Fig. 1. The program is entered on a punch card (Fig. 2) by punching holes at the appropriate places. The readoff unit is a set of contacts which are closed or opened (depending on the presence or absence of perforations in the punch card). The recorded information is time-separated discretely by commutator decatrons. The time count is made by the decatrons in strict synchronism with the power voltage. The maximum duration of a complete cycle is dependent upon the number of decatrons participating in program scanning. Further information enters a decoder, where it is converted into a stepped voltage by a clipper amplifier circuit. In addition to an output control voltage, the decoder issues various auxiliary commands, as well as a pressure program. The program of auxiliary operations and pressure is recorded on the same punch card.

Program-setting unit. The readoff unit consists of two contact panels in which spring contacts are mounted. The information recorded on a punch card may be presented in the form of a kind of matrix:

$$\begin{Vmatrix} a_{11} & a_{12} & a_{13} & \dots & a_{1n-2} & a_{1n-1} & a_{1n} \\ a_{21} & a_{22} & a_{23} & \dots & a_{2n-2} & a_{2n-1} & a_{2n} \\ a_{31} & a_{32} & a_{33} & \dots & a_{3n-2} & a_{3n-1} & a_{3n} \\ \dots & \dots & \dots & \dots & \dots & \dots & \dots \\ \dots & \dots & \dots & \dots & \dots & \dots & \dots \\ a_{m-11} & a_{m-12} & a_{m-13} & \dots & a_{m-1n-2} & a_{m-1n-1} & a_{m-1n} \\ a_{m1} & a_{m2} & a_{m3} & \dots & a_{mn-2} & a_{mn-1} & a_{mn} \end{Vmatrix}$$

where a_{ik} is a number that may assume only the value 0 or 1, in accordance with the presence or absence of a perforation on the program carrier. The value of n is determined from the formula

$$n = \frac{t_s}{T},$$

where $T = 2\pi/\omega$, and t_{ts} is the time of the welding cycle. The number m is determined from the formula $m = (k + 1) + q$. The quantity k is found from the expression

$$N = \sum_{k=0}^{k=m-1} a_k 2^k. \qquad (1)$$

The value of q corresponds to the number of supplementary busbars used to program the auxiliary operations.

Proceeding from technological requirements, we assign the smallest permissible increment of the welding current for one period to determine N. Let $(I_2 - I_1)/I_{max}\ 100\% = \Delta I/I_{max}\ 100\% = 7\%$, then $I_{max}/N\ 100\% = 7\%$. Hence N is easily found and the value of k is then readily determined from Expression (1).

The following numbers were selected for the present model: $k = 3$, $q = 2$ and, accordingly, $m = 6$.

Readoff of the information on an entire column is accomplished discretely at each moment n. Further conversion of the program is accomplished in the decoder, at the output of which the voltage takes a stepped form.

Time-scan circuit. The information time-scan circuit is constructed around Type A-101 commutator decatrons (Fig. 3). The cathodes of these decatrons have individual outputs which are not electrically connected with one another; therefore, at each moment of time $n = t/T$, current will flow through only one of the cathodes. The discrete time count, which is kept in synchronism with the power system, enables us to set the program cycles with absolute accuracy.

A triggering circuit which is connected to series of interlocks and auxiliary units is hooked up appropriately in accordance with the

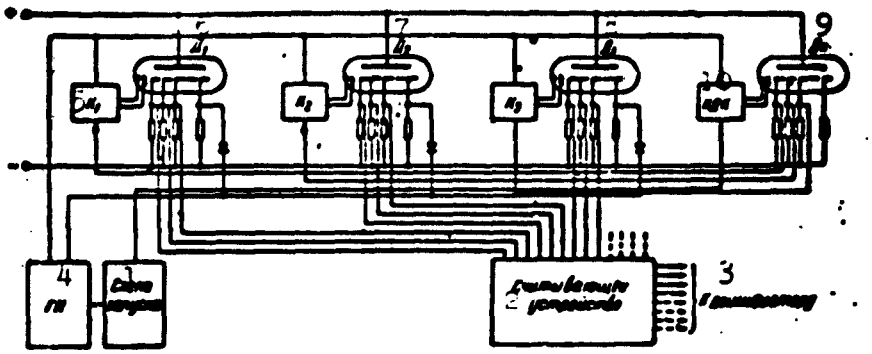

Fig. 3. Circuit of programming unit. 1) Triggering circuit; 2) readoff unit; 3) to decoder; 4) GI; 5) K_1, 6) D_1; 7) D_2; 8) D_3; 9) Dk; 10) KDK.

Fig. 4. Oscillogram of program output voltage.

purpose of the programming unit (for spot or seam welding).

At the moment the circuit is triggered, all the switches $K_2 \ldots K_k$, except for K_1 are closed. Counting pulses with a frequency of 100 cps, which are shaped by the special generator GI, pass through switch K_1 into the input circuit of the first decatron D_1. The discharge in the decatron, which is set up initially on a neutral cathode, begins to transfer through the subcathodes with the frequency of the triggering pulses onto the cathode row. At each moment of time n_1, a discharge is set up on only one cathode and the voltage drop across the cathode resistor is fed into the readoff unit. After the discharge reaches the ninth cathode, the voltage pulse is used to transfer the discharge of the commutator decatron DK to the second cathode. The voltage picked off the cathodes of the commutator decatron controls the switches $K_1 \ldots K_k$. On establishment of the discharge at the second cathode, the switch K_2 is opened and K_1 closed. Reading pulses from the generator GI begin to proceed to the second decatron D_2. The reading continues

in the same manner. On completion of the welding cycle, the last impulse sets the commutator decatron DK to its initial state and in this way prepares the circuit for the next cycle.

In seam welding, the cycle is repeated automatically, and both manual and automatic control are provided for spot welding.

The readoff unit distributes the incoming signal from the decatrons in accordance with the program recorded on the punch card among the busbars m, each of which corresponds to a number $a_{ki}2^0$, $a_{ki}2^1$, $a_{ki}2^2$,..., $a_{ki}2^k$. The coefficients a_{ki} acquire the values 0 or 1 depending on whether there is a hole in the punch card.

Decoder circuit. The voltage taken from the cathodes of the decatrons is fed through the reading unit to the decoder. In the decoder, the recorded code is converted into a step voltage which is the main output of the apparatus. The shape of the output voltage is shown on the oscillogram (Fig. 4).

The decoder is a device which consists of a row of transistorized clipper amplifiers (their number depends on N). The current proceeding from each clipper amplifier through the common resistor R_0 is an algebraic sum of the form

$$\sum_{i=1}^{S} I_{k_i} = I_1 + I_2 + I_3 + \ldots + I_S, \qquad (2)$$

where I_i is the current from the i^{th} clipper amplifier, and S is the number of clipper amplifiers, which is determined from $N = \sum_{k=0}^{k=n-1} a_k 2^k$ as $S = k + 1$.

The voltage drop across the resistor R_0 is the output voltage and thereafter controls the operation of the phase rotator.

The programming unit developed, like the one described in [1], may be used to set the electrode-pressure program in spot welding and in certain auxiliary operations.

The design and compilation of the program are not difficult and are accomplished by a production engineer on the basis of corresponding tables [1] without using computing machines.

CONCLUSIONS

1. An apparatus was developed which enables us to record a program on a fixed punch card and thereby obviates the use of movable elements for program reading.

2. The application of decatrons enables us to count time more reliably and to repeat a program immediately after completion of a given cycle.

3. The circuit developed has a smaller number of tubes and differs from earlier circuits in having a simpler design.

REFERENCES

1. B.Ye. Paton, V.S. Gavrish and Yu.S Grodetskiy, Universal'noye programiruyushcheye ustroystvo [Universal Programming Device], Avtomaticheskaya svarka [Automatic Welding], No. 7, 1961.

Submitted 19 January 1962

[List of Transliterated Symbols]

Manuscript Page No.	
1	СУ = SU = schityvayushcheye ustroystvo = readout unit
1	БРП = BRP = blok razvertki programmy = program scan unit
1	Д = D = deshifrator = decoder
1	пр = pr = programm = program
3	ц = ts = tsikl = cycle
4	К = K = klyuch = switch
4	Д = D = dekatron = decatron
4	ГИ = GI = generator impul'sov = pulse generator
4	ДК = DK = dekatron, kommutatornyy = commutator decatron

WELDABILITY OF 30KhSNVFA HARDENING SHEET STEEL IN DOUBLE AND SINGLE-SIDED, DOUBLE-PASS ARGON-SHIELDED ARC WELDING

S.L. Mandel'berg and V.G. Gordonnyy

(Order of the Red Banner of Labor
Electric Welding Institute imeni Ye.O. Paton,
Acad. Sci UkrSSR)

This report presents the results of a comparative investigation of double-sided welding and a new technique of double-pass, one-side argon-shielded welding of type 30KhSNVFA steel in thicknesses of 1.5, 2.2 and 4.0 mm.

High-strength Type 30KhSNVFA hardening sheet steel, like other steels of this type, is usually welded in an argon medium with a nonconsumable tungsten electrode. The procedure of single-pass welding on copper backing with welding wire of composition close to the base metal fed into the arc zone had come into preferred use. This procedure is afflicted with serious drawbacks and in many cases does not guarantee a welded joint of the required quality. Two-sided welding using a nonconsumable electrode without filler wire gave better results. However, even this procedure often fails to guarantee the necessary crack resistance in the welded joints. A further disadvantage of the procedure is the increased amount of labor required.

The purpose of the present work was to make a comparative investigation of the known double-sided welding procedure and the new double-pass argon-shielded welding procedure on type 30KhSNVFA steel. In the new procedure [1], the seam consists of two layers (Fig. 1). The second layer completely covers the first, but the depth of its

Fig. 1. Double-pass single-side seam.

penetration does not exceed 60-70% of the thickness of the welded sheets. To impart this shape to the penetration for the second layer when welding metal less than 2.0-2.2 mm thick, a tungsten electrode is moved across the seam with a certain frequency and amplitude.

In the investigation, a set of specimens of the type of steel indicated above with thicknesses of 1.5, 2.2 and 4.0 mm were welded

TABLE 1

Conditions of Double-Pass Single-Side and Double-Side Argon-Shielded Welding of Type 30KhSNVFA Steel

1	2	3	13	4	5	6	7	8	9	10
Вариант технологии сварки	Толщина металла, мм	№ слоя	$I_{св}$, а	$U_д$, в	$V_{св}$, м/час	Диаметр присадочной проволоки, мм	$V_{п.э}$, м/час	Расход аргона, л/мин	Частота колебаний электрода в секунду	Амплитуда колебаний электрода, мм
11	1,5	1	120	9	20	—	—	8	—	—
		2	100	8	20	1.2	20	8	4—6	2,0—2,5
Односторонняя двухслойная	2,2	1	120	9	11	—	—	8	—	—
		2	110	8	12	1,4	12	8	4—6	2,0—2,5
	4,0	1	160	10	8	2,0	12	10	—	—
		2	200	10	12	2,0	28	10	—	—
12	1,5	—	90	8	24	—	—	8	—	—
Двухсторонняя	2,2	—	110	8	20	—	—	8	—	—
	4,0	—	240	10	12	—	—	10	—	—

Notes: 1) Welding was accomplished with a tungsten electrode with a diameter of 3 mm. 2) The double-sided seams were welded under the same conditions from the inside and outside.

1) Variant of welding procedure; 2) thickness of metal, mm; 3) layer No.; 4) U_d, V; 5) V_{sv}, m/hour; 6) diameter of filler wire, mm; 7) $V_{p.e}$, m/hour; 8) argon input, liters/min; 9) vibration frequency of electrode in seconds; 10) vibration amplitude of electrode, mm; 11) single-side double-pass; 12) double-sided; 13) I_{sv}, amp.

with double-sided and double-pass single-sided seams. The conditions under which the specimens were welded are given in Table 1.

The mechanical properties, the structure of the welded joints and the composition of the seam metal were investigated. Crack re-

sistance was studied with the use of special specimens and on macrosections. It was established that the seam-metal composition differed from that of the base metal by having 0.02-0.03% less carbon and 0.01-0.02% less of other elements.

The mechanical properties of the joints were determined after heat treatment of the welded specimens (hardening and tempering or isothermal hardening and tempering) by testing flat tensile specimens and impact-bending specimens with notches along the seams. The specimens were prepared in conformity with GOST 6996-54 (Type IX and Type VII). For comparison, base-metal specimens of the same size were subjected to the shock-bending test.

The tests showedthat failure occurred in the base metal in all cases with the variants of the procedure that we compared. The impact strength of the seam metal was equal to or somewhat greater than that of the base metal.

In tensile testing a second series of flat specimens, on which the small reinforcements resulting from the argon-shielded welding were completely ground down, failure occurred in the base metal far from the seam as in the tests with the reinforcements unground.

These results showed that in spite of a certain reduction in the content of hardening admixtures, the seam metal had a higher strength than the base metal. We should assume that in the present case, the strength increases due to the structural characteristics of the seam metal and its high purity, which is attained as a result of remelting of the metal during welding in the argon medium. Submerged-arc welding [2] and molten-slag arcless electric remelting of metal with consumable electrodes [3] produced similar results.

The causes of the increase in the strength of the remelted metal and the improvement of its other properties are the subjects of an in-

dependent investigation.

Metallographic investigations showed that subsequent to heat treatment, the seam metal and the metal around the weld zone have a troostite structure which differs little from that of the base metal.

Various types of special rigid specimens are used [4] to evaluate the crack resistance of the seam metal and the metal around the weld zone in alloy steels. Most of them can be used only to investigate the weldability of metal in comparatively large thicknesses. The familiar H specimens (Fig. 2), as well as those in which stresses of varying magnitude are created by varying the rigidity of the specimen mount (Fig. 3), were the most suitable for metal with the thicknesses (1.5-4 mm) that we were investigating. These specimens simulate the highly unfavorable conditions prevailing in welding of real joints (closed contours and intersections of welds).

The H specimens were welded from steel plates with thicknesses of 1.5, 2.2 and 4.0 mm. The auxiliary fastening seams which are keyed 1 and 3 in Fig. 2 were welded in two layers (double-pass single-sided welding) or on two sides (double-sided welding). The control seam 2, the welding results of which were used to evaluate crack resistance, was made by the version of procedure that we were investigating after complete cooling of the fastening seams. The penetration shape of the control seams that were made under the conditions indicated in Table 1 is shown in Fig. 4. The control seam was welded from the back side or with a second layer only in cases where visual examination turned up no cracks in the seam 24 hours after the first layer was welded.

The results of comparative evaluation of the steel's crack resistance based on welding of the H-shaped specimens are given in Table 2, from which it is apparent that a much higher crack resistance in the metal is guaranteed with single-sided double-pass welding.

Cracks did not form in the specimens produced by double-pass single-sided welding where steel with thicknesses of 1.5 and 2.2 mm was welded. At the same time, cracks formed immediately after welding in the single-sided seam of a double-pass joint in steel with a thickness of 2.2 mm. They were detected in steel specimens 1.5 mm thick only on macrosections. In welds in metal 4.0 mm thick, the high crack resistance after single-sided double-pass welding is apparent from the fact that with this procedure, cracks form 30 to 50 minutes after welding, while they form in 1 to 2 minutes where double-pass welding is used.

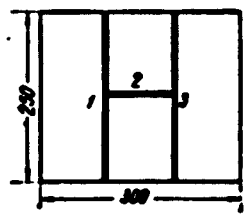

Fig. 2. H-shaped specimen used to determine crack resistance of seam.

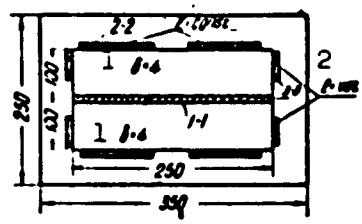

Fig. 3. Specimen used to determine crack resistance; different rigidities obtained by varying size of side tack welds. 1) b = 4.

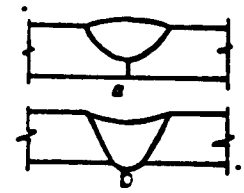

Fig. 4. Shape of first seam. a) With double-sided welding; b) with single-sided double-pass welding.

To confirm the data obtained, the crack resistance in metal with a thickness of 4.0 mm was checked on the specimens shown in Fig. 3 by the following method. Two plates with the dimensions 4 x 100 x 250 mm were placed on a steel slab with a thickness of 30 mm. The edges 1-1 (Fig. 3) which were welded in conformity with the procedure under study were fitted tightly to one another. The plates were welded to the slab manually along the edges 2-2. To create stresses of different magnitudes, the lateral seams 3-3 were laid manually in varying lengths (10, 20, 30, 40 mm and so forth). After preparation, the specimens were joined by the double-pass or double-sided welding procedure (Table 1). During the welding process and for the next 24 hours, the specimens

were subjected to systematic examination. A total of 12 specimens were welded. Cracks formed along the center of the seam in the six specimens made by double-pass welding where the length of the lateral tack welds were 50 to 60 mm. Cracks appeared in the seams made by double-sided welding even in the absence of lateral tack welds.

TABLE 2

Results of Determination of Seam Metal Resistance to Cracking (H-shaped specimens)

1 Толщина сварного металла, мм	2 Вариант технологии сварки	3 Количество сварных образцов	4 Время от окончания сварки до образования трещин в первом шве	5 Трещины в макрошлифах после сварки второго шва: количество шлифов	7 шлифов с трещинами
1,8	8 Двухслойная односторонняя	12	10 Нет трещин	48	Нет 14
	9 Двухсторонняя	12	» »	48	0
2,2	Двухслойная односторонняя	12	Нет трещин	—	—
	Двухсторонняя	12	Трещины через 11 30—50 сек.	—	—
4,0	Двухслойная односторонняя	6	Трещины через 12 30—50 мин.	—	—
	Двухсторонняя	6	Трещины через 13 1—2 мин.	—	—

Notes: 1) Cracks formed along the center of the seam. 2) In cases where cracks were detected on visual examination, macrosections were not prepared. 3) Metal specimens of a given thickness were prepared from steel of the same melt for the double-sided and double-pass single-sided seams.

1) Thickness of welded metal, mm; 2) variant of welding procedure; 3) number of specimens welded; 4) time from completion of welding to formation of cracks in first seam; 5) cracks in macrosections after welding of second layer; 6) number of sections; 7) sections with cracks; 8) double-pass single-sided; 9) double-sided; 10) no cracks; 11) cracks after 30-50 seconds; 12) cracks after 30-50 minutes; 13) cracks over period of 1-2 minutes; 14) none.

Additional experiments were conducted welding H-shaped specimens at the same welding speed with double-sided and single-sided double-pass seams. These experiments again showed that much higher crack resistance is guaranteed in joints with double-pass single-sided seams.

The experiments conducted enable us to draw the conclusion that

double-pass single-sided welding of type 30KhSNVFA steel in thicknesses of 1.5 to 4.5 mm guarantees a higher crack resistance in the metal than is attained with double-sided welding. The reason for this, in our opinion, consists in the fact that an unpenetrated zone (Fig. 4) which plays the role of a stress concentrator is retained in a double-sided joint after welding of the first seam. In addition to this, on welding, the section of such a seam is smaller than that of the first layer of a double-pass single-sided joint. Therefore, such seams are less resistant to cracking.

REFERENCES

1. S.L. Mandel'berg and V.G. Gordonnyy, Odnostoronnyaya dvukhsloynaya argono-dugovaya svarka tonkolistovoy legirovannoy stali [Single-Sided Double-Layer Argon-Shielded Arc Welding of Sheet Alloy Steel], Avtomaticheskaya svarka [Automatic Welding], No. 9, 1961.
2. A.M. Makara, Osobennosti svarki vysokoprochnykh staley [Special Features of the Welding of High-Strength Steels], Sbornik materialov nauchno-tekhnicheskogo soveshchaniya [Collection of Data of the Scientific-Technical Conference], MDNTP, 1959.
3. Povysheniye kachestva legirovannykh staley putem elektroshlakovogo pereplava [Increasing Quality of Sheet Steel by Molten-Slag Arcless Electric Welding], Edited by B.Ye. Paton, Mashgiz, 1960.
4. A.I. Krasovskiy, Sposoby ispytaniy konstruktsionnykh staley na svarivayemost', primenyayemyye v SSSR i za rubezhom [Methods for Weldability Testing of Structural Steel Used in the USSR and Abroad], VINITI, 1959.

Submitted 1 August 1961

Manuscript Page No.	[List of Transliterated Symbols]
8	св = sv = svarka = welding
8	д = d = duga = arc
8	п.э. = p.e. = podacha elektroda = electrode feed

ALLOYING OF HEAT-RESISTING AUSTENITIC STEELS, ALLOYS AND WELDED SEAMS WITH BORON IN THE 0.3-1.5% RANGE

B.I. Medovar, L.V. Chekotilo, V.A. Lutsyuk-Khudin, N.I. Pinchuk and L.G. Puzrin

(Order of the Red Banner of Labor Electric-Welding Institute imeni Ye.O. Paton, Acad. Sci. UkrSSR)

It is shown that boron-alloyed austenitic heat-resisting steels and alloys, having a two-phase structure – austenite and a boride component of eutectic origin –, are characterized by high long-term strength and plasticity. The presence of the two-phase structure predetermines the absence of around-the-weld hot (crystallization) cracks and the elevated resistance of welded joints to local failure along the interface between the base metal and seam during operation or heat treatment.

Alloying of seam metal with boron renders the metal resistant to the formation of crystallization cracks and sharply increases the heat resistance without loss of long-term plasticity.

1. Until recently, boron was introduced into the composition of austenitic steels and alloys in small quantities, generally measured in hundredths of a percent, for the purpose of achieving some improvement in the technological properties and heat resistance of these materials [1, 2, 3, and other sources]. The development of atomic industry and power engineering has brought with it the development of a new group of stainless austenitic steels containing up to 1.5-2.0% B [4 and other sources].

Austenitic steels alloyed with boron are used, as a rule, at

temperatures below 350-400°, i.e., they are essentially heat-resisting structural materials. Meanwhile, it is reported [5,6] that non-corrosive boron steels have been subjected to precipitation hardening at rather high temperatures – approximately 800°. Thus, for example, after four hours of aging at this temperature, the hardness of an austenitic steel with 1.14% B increased from 250 to 450 HB and remained at this level under prolonged aging.

The high precipitation temperature of the hardening phase – in this case, the boride phase – predetermines the feasibility of using high-boron stainless steels as heat-resisting materials.

In spite of this, insufficient attention is given to the problems of increasing the heat resistance of austenitic steels with the aid of boron employed as an alloying element. We may note among the studies in this field that are known to us the papers of the Japanese [20, 22] investigators who established the possibility of increasing the heat resistance of type Kh18N12 steel by introduction of 0.17% B. Together with this, data of English investigators, which would indicate a reduction in the effectiveness of the influence of boron on heat resistance where its concentration in steel is above 0.10-0.15% are given in Reference [1]. Similar conclusions were also drawn in the USSR ten years ago [6]. In connection with this, particular interest is attracted to the data of Kraft and Flinn [8], which were published in the USA and mentioned in a paper by German investigators [7], relating to a substantial increase in the heat resistance of austenitic cast steels containing up to 5% B at temperatures right up to 815°. It is noted in a number of reports that boron and silicon [20, 21] maintain the high-temperature corrosion resistance and plasticity of steels and alloys with a simultaneous increase in heat resistance.

2. The particular interest of welders in boron as an alloying

element rather than a minor additive is explained by the following.

It is known that when heat-resisting austenitic steels and alloys are welded, we risk the appearance of hot (crystallization) cracks not only in the seam metal, but also in the around-the-weld zone [9, 10].

It is possible to counter hot cracks in austenitic seams by active intervention in the primary crystallization process of the welding pool [10 and other sources], and occasionally even with the nature of the force field [11].

It is considerably more complex to prevent the formation of around-the-weld intergranular cracks. In Reference [12], we showed that the principle role in the solution of this problem belongs to the metallurgists, although welders occasionally succeed in eliminating around-the-weld cracks. Here we refer, for example, to healing of these cracks by the relatively low-melting metal of the welding pool [13]. As was established in welding of nickel, we may use a zirconium [9]- or boron-rich eutectic component as the low-melting liquid. The boride phase acts rather effectively, healing around-the-weld cracks even in welding of austenitic steels and alloys (Fig. 1).

It has been established that a radical means of preventing hot cracks in austenitic seams is to change the seam composition in such a way as to form a two-phase primary structure [10]. As applied to heat-resisting steels, the use of δ-ferrite as the second phase is undesirable in view of the danger of embrittling the metal as a result of the $\delta \rightarrow \sigma$ transformation in more or less long-term operation.

Hot cracks in seam metal are effectively prevented, for example, by a phosphide or sulfide eutectic present in the metal in sufficient quantity [14]. But such seams are naturally not permissible in heat-resistant designs due to the low melting point of the second phase.

Fig. 1. Around-the-weld crack healed by boride eutectic. 1Kh14N18V2BR (EI726) steel 0.17% B in seam (600X).

The boride phase is interesting to welders precisely for the reason that, while having the characteristic ability of all eutectic phases to prevent cracks in seams, the boride phase is further distinguished firstly by a relatively high melting point and, secondly, it is not subject to a transformation capable of causing metal embrittlement in the process of prolonged joint interaction of operating temperatures and loads. As we see, for these reasons alone we should have begun long ago to give attention to the boride phase and resort to alloying austenitic seams with boron.

It has been shown repeatedly in a series of studies by Soviet and foreign investigators that boron should be considered a harmful – from the welding standpoint – impurity in various steels, including the austenitic steels [10, 15, 16 and other sources]. At first glance, therefore, the recommendation that boron be used as a means of preventing cracks when welding austenitic steels may seem strange. There is, however, no contradiction in this. Crystallization cracks form in the presence of small quantities of the low-melting liquid on the boundaries of the crystals and do not form where there is a rather high eutectic content [14]. For melts classified as solid solutions with limited solubility, the curve of seam hot-shortness versus the concentration of the low-melting phase always has a maximum. On either side of the maximum, i.e., when there is a very small or, on the other hand, a rather high content of a given phase or element, there is no danger of the appearance of hot cracks.

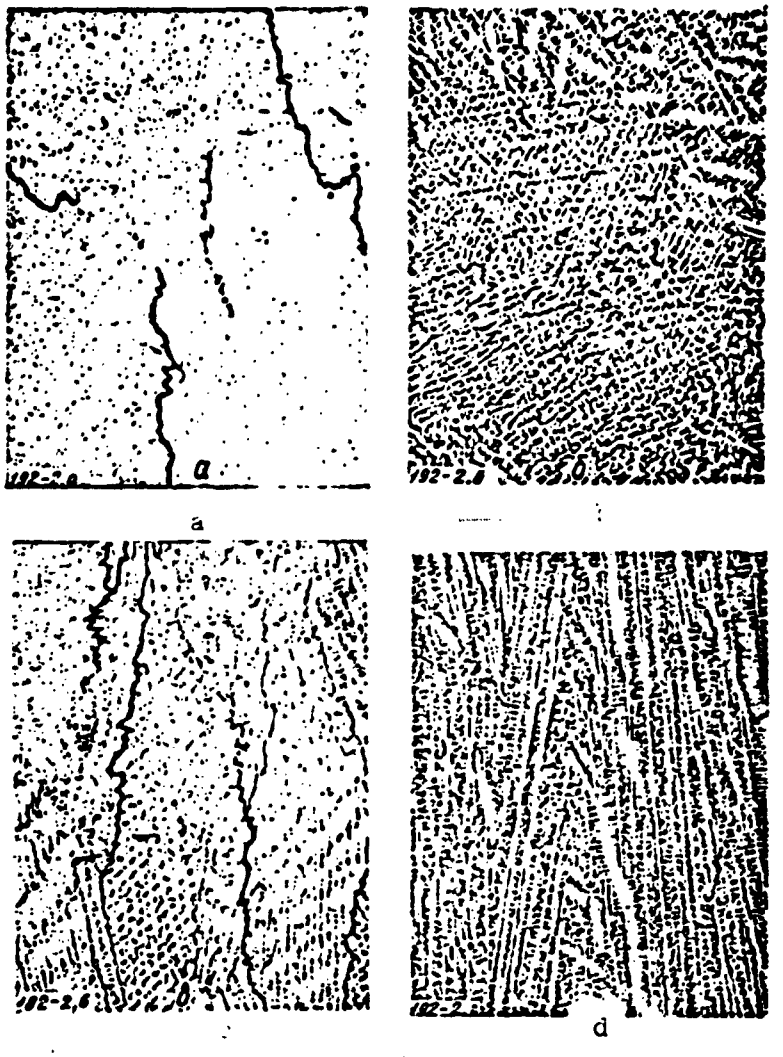

Fig. 2. Prevention of hot (crystallization) cracks in austenitic seams (70X). a) Seam without boron on 1Kh15N35V5T (EI725) alloy, cracks present; b) same, 0.51% B in seam, no cracks; c) seam without boron on 1Kh18N11B (E1402) steel, cracks; d) same, 0.53% B in seam, no cracks.

Thus, boron in large concentrations can increase the resistance of austenitic seams to hot cracks (Fig. 2) considerably. In addition to this, the introduction of boron is helpful for the purpose of preventing around-the-weld cracks. Boron not only heals cracks, as has already been mentioned, but it also contributes to the formation of a two-phase structure in the around-the-weld zone (Fig. 3). Here, we

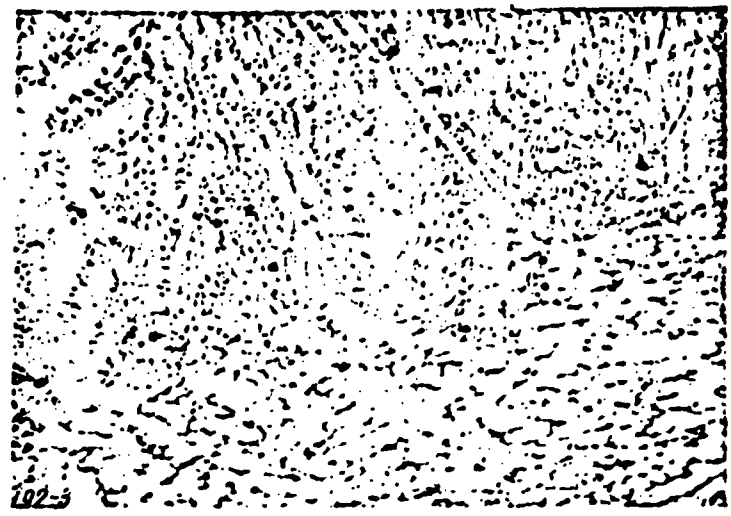

Fig. 3. Absence of around-the-weld cracks in welding two-phase austenitic Kh18N15M3BR steel with 0.45% B (120X).

should recall that the presence of the two-phase ($\gamma + \delta$) structure in the around-the-weld zone is one of the most effective methods of preventing cracks in metal directly at the junction line [17].

3. Recently, apart from the problems under consideration (the prevention of hot cracks in and around seams), another no less serious problem has arisen without correct solution of which further progress in the creation of reliably performing weld designs from austenitic heat-resisting steels and alloys is impossible. We refer here to the so-called local failure of welded austenitic steel joints which occurs in the around-the-weld zone at a distance of one or several grains from the interface between the base metal and seam. This problem is analyzed in the paper of B.I. Medovar and V.A. Lutsyuk-Khudin [18].

The common nature of the causes of the tendency of austenitic steels to knife corrosion and local failure was established in the first stage of the investigations. It was suggested on this basis that we resort to the same means which were proven effective in preventing knife corrosion [18] in order to prevent local failure in

austenitic steels. Subsequent experiments enabled us to broaden our ideas concerning this dangerous phenomenon. It was found that intercrystalline cracks which develop in the vicinity of the junction line over a period of many hundreds and thousands of hours of operation often originate in those zones of the austenite-grain boundaries which were partially melted in the very welding process. A comparatively large quantity of boron in steel (for example, 0.015-0.020%) leads to local flashing off of the grain boundaries (Fig. 4a) and to formation of hot cracks which may become the seats of the ensuing local breakdown. A similar phenomenon is also observed in the around-the-weld zone on welding high-nickel steels and alloys alloyed with titanium (Fig. 4b and c; in this case, apparently a nickel-titanium eutectic may form on the grain boundaries).

It was natural to assume that welded joints of austenitic steel alloyed with boron should not be susceptible to local failure. The following considerations speak in favor of this assumption: firstly, the absence of the seats of ensuing breakdown in the form of hot (crystallization) around-the-weld cracks; secondly, the absence of carbide hardening of the grain boundaries in boron austenitic steel and hence the constancy of the carbide-phase composition through the temperature-force disturbance imposed by the welding heat cycle in the overheated region of the around-the-weld zone [18].

Our hypotheses were fully confirmed when composite specimens were welded for quick evaluation of the tendency of austenitic steels to local failure in the around-the-weld zone: none of the tested boron austenitic steels containing more than 0.35% B was found subject to this type of failure (Table 1, Fig. 5).

Thus, it is also desirable to resort to the use of boron as an alloying element in heat-resisting austenitic steels for the purpose

Fig. 4. Local flashing off of boundaries of austenitic grains in welding of austenitic heat-resisting steels. a) EI726 steel with 0.020% B, boride eutectic (1200X); b) EI696 steel with 0.015% B and 3.07% Ti, titanium-rich phase (1000X); c) EI725 with 0.005% B and 1.36% Ti, titanium-rich phase (1000X).

of preventing local brittle failure of welded joints.

4. We have already stated that the high-temperature precipitation hardening of boron austenitic steels governs the possibility of increasing the heat resistance of austenitic steels with the use of high boron concentrations. The corresponding data of the authors are given in Table 2; for comparison, the same table gives the data obligingly provided to us by Professor G.V. Estulin and engineer L.Ye. Ivanova.

TABLE 1

Influence of Boron on Tendency of Heat-Resisting Austenitic Steels to Local Breakdown (tested by accelerated method)

1 Тип стали	2 Марка стали	Содержание бора, %	Склонность к локальному разрушению	5 Примечание
1Х14Н18В2Б 6	ЭИ695 12	0	Нет 17	Отсутствие разрушения обусловлено высоким соотношением Nb:C
1Х14Н18В2БР 7	ЭИ726 13	0,015	Есть 18	Локальное разрушение обусловлено недостаточно высоким соотношением Nb:C
1Х18Н11Б 8	ЭИ402 14	0	»	
1Х18Н11БР 9	Опытная 15	0,40	Нет 19	
Х18Н15 10	ЭИ846 16	0,27	Есть 18	Рис. 5, а 21
		0,37	Нет 17	
		0,53	»	
		0,69	»	Рис. 5, б 22
Х18Н15М3БР1 11		0,36	»	

1) Type of steel; 2) brand of steel; 3) boron content, %; 4) tendency to local failure; 5) remarks; 6) 1Kh14N18V2B; 7) 1Kh14N18V2BR; 8) 1Kh18N11B; 9) 1Kh18N11BR; 10) Kh18N15; 11) Kh18N15M3BR1; 12) EI695; 13) EI726; 14) EI402; 15) experimental; 16) EI846; 17) none; 18) some; 19) absence of failure due to high Nb:C ratio; 20) local failure due to inadequate Nb:C ratio; 21) Fig. 5a; 22) Fig. 5b.

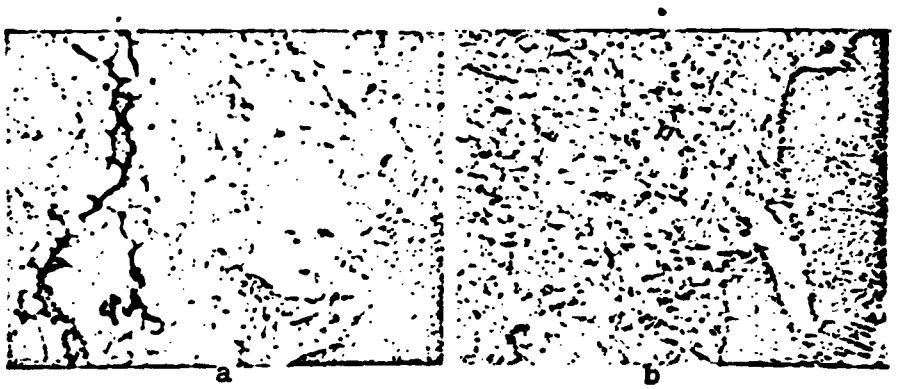

Fig. 5. Prevention of local failure in around-the-weld zone in welding austenitic heat-resisting steels (70X). a) Steel with 0.27% B, local failure; b) steel with 0.69% B, no local failure.

It was found that boron sharply increases the heat resistance of welded seams (Table 3). Thus, for example, the introduction of 0.41% B into a Kh18N11B seam enables us to nearly double its hundred-hour strength at 650° (from 20 to 36 kgf/mm^2) or to increase the time to

TABLE 2

Influence of Boron on Heat Resistance of Austenitic Steels

1 Тип металла шва	2 Содержание бора, %	3 Температура испытания, °С	4 Напряжение, кгс/мм²	5 Время до разрушения, ч	δ, %	ψ, %	6 Примечание
1Х18Н15 7	0	650	10	239	11.6	14,1	Данные Г. В. Эстулина и Л. Е. Ивановой 13
1Х18Н15Р 8	0,5			1117	31,2	32,4	
1Х18Н15Р1 9	0,8			1387	33.7	40,5	
1Х18Н15Р2 10	2,0			6728	54,0	51,2	
1Х18Н15 7	0	800	3	335	10,4	13,2	
1Х18Н15Р 8	0,5			544	24,8	29,2	
1Х18Н15Р1 9	0,8			987	23,6	19,6	
1Х18Н15Р2 10	2,0			1986	36,4	35,6	
Х16Н15 11	0.15	600	24	130	33.7	31,1	Данные авторов 14
Х16Н15Р1 12	0.50			260	26,3	36,0	

1) Type of seam metal; 2) boron content, %; 3) test temperature, degrees; 4) stress, kgf/mm^2; 5) time to failure, hours; 6) remarks; 7) 1Kh18N15; 8) 1Kh18N15R; 9) 1Kh18N15R1; 10) 1Kh18N15R2; 11) Kh16N15; 12) Kh16N15R1; 13) data of G.V. Estulin and L.Ye. Ivanova; 14) data of authors.

TABLE 3

Influence of Boron on Heat Resistance of Austenitic Welded Seams

1 Тип металла шва	2 Содержание бора, %	3 Температура испытания, °С	4 Напряжение, кгс/мм²	5 Время до разрушения, ч	δ, %	ψ, %	6 Примечание
1Х18Н11Б 7	0	650	20	100	—	—	По ТУ 15
1Х18Н11БР 8	0,41	650	20	1300[1]	—	—	
			26	919	8,2	38,3	
			32	334	15,4	22,5	
			36	90	10,3	31,1	
1Х18Н11БР1 9	0,9	650	20	624[1]	—	—	
			26	1045	6,3	19,0	
			32	290	6,0	16,5	
			36	150	6,4	20,8	
1Х15Н35Г7В3Т 10	0	800	6	100	31,6	49,0	
1Х15Н35Г7В3ТР 11	0,56	800	6	400[1]	—	—	
			8	90	24,3	70,1	
1Х15Н35Г7В7М3Т 12	0	800	7	835	14,8	30,5	
			10	214	18,7	46,5	
			12	20	21,1	75,6	
1Х15Н35Г7В7М3ТР1 13	1,3 (по расчету) 14	800	7	960[1]	—	—	
			10	417	10,3	23,1	
			12	78	14,2	24,6	

Note: 1) Intact after test.

1) Type of seam metal; 2) boron content, %; 3) test temperature, degrees; 4) stress, kgf/mm^2; 5) time to failure, hours; 6) remarks; 7) 1Kh18N11B; 8) 1Kh18N11BR; 9) 1Kh18N11BR1; 10) 1Kh15N35G7V3T; 11) 1Kh15N35G7V3TR; 12) 1Kh15N35G7V7M3T; 13) 1Kh15N35G7V7M3TR1; 14) (from calculation); 15) on basis of technical specifications.

failure at this temperature and a stress of 20 kgf/mm^2 from 100 to 1000 hours, i.e., by a factor of ten. We also obtained similar data when testing Type Kh15N35 welded seams.

Our attention is drawn to the fact that the sharp increase in heat resistance is accompanied by a striking increase in long-term plasticity.

5. The welding of austenitic boron steels that contain up to 0.8 - 1.0% B and belong to the class of hypoeutectic steels does not cause difficulty. In welding steels with a larger quantity of boron, the danger of the formation of cold cracks, which result from reduced plasticity due to the significant quantity of the eutectic phase, is increased. Austenitic steels of this type, particularly in rigid designs or assemblies, must be welded hot, with retarded cooling, to avoid cold cracks. The composite specimens (Fig. 6) had, for example, to be welded in a furnace heated to 800° with subsequent cooling to room temperature over a period of 12 hours. In passing, we should note that the presence of 10% B in the seam metal reduces the danger of damage by hot cracks which originate from the spaces between the "piano keys" (Fig. 7).

6. Alloying with boron increases the long-term plasticity of austenitic steels, but is accompanied by a noticeable reduction in the plastic properties of the metal, and in the impact strength in particular. In the hot state, boron steels do not deform as well as those without boron. The manufacture of seamless pipes from steels alloyed with boron and occasionally even the preparation of rolled sheet are linked with certain difficulties. Here, a new means of increasing the plasticity, particularly the hot plasticity of austenitic steels - molten-slag arcless electric remelting of consumable electrodes in a metallic water-cooled crystallizer - has been of

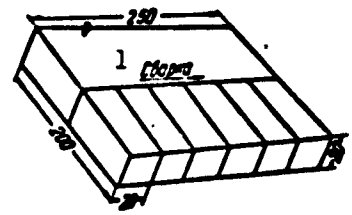

Fig. 6. Composite specimen used to evaluate tendency of welded seam to form hot cracks originating from spaces between "keys." 1) Welding.

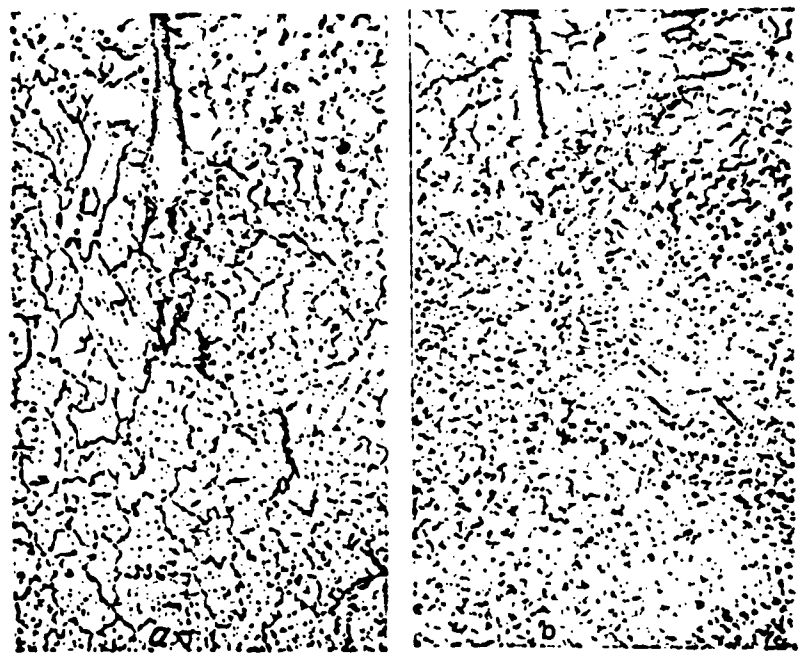

Fig. 7. Influence of boron on formation of hot cracks originating from spaces (EI868 alloy) (70X). a) No boron in seam, crack; b) 1.0% B in seam, crack did not develop.

help [19].

CONCLUSIONS

1. The alloying of austenitic steels and seams welded on these steels with boron (over 0.3-0.4%) enables us to solve the following most important problems: to increase the resistance of the seam metal to the formation of hot (crystallization) cracks sharply; to eliminate

almost entirely the danger of the appearance of around-the-weld hot cracks on welding; to guarantee extremely high reliability in welded joints, which operate for long periods under conditions of the joint influence of temperatures and loads due to the elimination of factors capable of giving rise to local brittle failure in the around-the-weld zone.

2. The above problems are solved with a substantial simultaneous increase in the heat resistance of the austenitic steels and welded seams.

REFERENCES

1. M.V. Pridantsev and K.A. Lanskaya, Stali dlya kotlostroyeniya [Steels for Boiler Construction], Metallurgizdat [State Scientific and Technical Publishing House for Literature on Ferrous and Nonferrous Metallurgy], 1959.
2. W.E. Blatz, E.E. Reymonds and W.W. Dyrkacz, Symposium on Metallic Materials for Service at Temperatures above 1600° F, No. 174, 1955.
3. Y.T. Brown and Y. Bulina, A New Higher-Temperature Turbine Disk Alloy, High Temperature Materials, No. 7, 1959.
4. Materialy komissii po atomnoy energii SShA. Yadernyye reaktory [Data of Atomic Energy Commission of the U.S.A. Nuclear Reactors], IL [Foreign Literature Publishing House], Moscow, 1956.
5. E. Gudremon, Spetsial'nyye stali [Special Steels], Vol. 2, Metallurgizdat, 1960.
6. V.M Prosvirin, N.S. Kreshchanovskiy and E.S. Ginzburg, Vliyaniye bora na strukturu i svoystva austenitnoy stali [The Effect of Boron on the Structure and Properties of Austenitic Steel], in book entitled Voprosy metallovedeniya austenitnykh staley [Problems of the Physical Metallurgy of Austenitic Steels], Book 52, Mashgiz [State Scientific and Technical Publishing House of Literature on Machinery], 1952 (TsNIITMASh) [(Central Scientific Research Institute of Technology and Machinery)].
7. K. Bungardt and R. Oppenheim, Eigenschaften nichtrostender austenitischer Chrom-Nickel Staehle mit Bor fuer den Kernreaktoren [Properties of Stainless Austenitic Chrome-Nickel Steels with Boron for Nuclear Reactors], Archiv fuer das Eisenheuttenwesen [Arch. Met. Iron], Vol. 32, No. 2, 1961.
8. R.W. Kraft and R.A. Flinn, Transactions of American Society for

Metals, 52. (1959); Vorabdruck [Preprint], No. 133, 175, Nickel Berichte [Nickel Reports], 17 (1959), page 343.

9. B.I. Medovar, O mekhanizme obrazovaniya okoloshovnykh mezhkristallicheskikh treshchin pri svarke plavleniyem [The Mechanism of the Formation of Around-the-Weld Intergranular Cracks in Fusion Welding], ZhTF [Journal of Technical Physics], Vol. 27, No. 7, 1957.
10. B.I. Medovar, Svarka khromonikelevykh austenitnykh staley [The Welding of Chrome-Nickel Austenitic Steels], Mashgiz, 1958.
11. B.I. Medovar and L.V. Chekotilo, Odnoprokhodnaya svarka stabil'no-austenitnykh staley [Single-Pass Welding of Stable-Austenitic Steels], in collection entitled Mashinostroyeniye [Machine Building], No. 3, izd. ININ GK KNIR USSR [Unlisted].
12. B.I. Medovar, L.V. Chekotilo, N.I. Pinchuk and V.A. Lutsyuk-Khudin, Mezhkristallicheskiye okoloshovnyye treshchiny pri svarke austenitnykh staley i splavov [Intergranular Around-the-Weld Cracks in the Welding of Austenitic Steel and Alloys], Svarochnoye proizvodstva [Welding Practice], No. 4, 1962.
13. N.F. Lashko and S.V. Lashko-Avakyan, Svarivayemyye legkiye splavy [Weldable Light Alloys], Sudpromgiz [State All-Union Publishing House of the Shipbuilding Industry], 1960.
14. B.I. Medovar, K voprosu o prirode goryachikh treshchin v svarnykh shvakh [The Problem of the Nature of Hot Cracks in Weld Seams], Avtomaticheskaya svarka [Automatic Welding], No. 4, 1954.
15. D.M. Rabkin and I.I. Frumin, Prochiny obrazovaniya goryachikh treshchin v svarnykh shvakh [Causes of the Formation of Hot Cracks in Weld Seams], Avtomaticheskaya svarka, No. 2, 1950.
16. A.V. Russiyan and M.Kh. Shorshorov, Vliyaniye bora na sklonnost' zharoprochnykh austenitnykh staley tipa 1Kh13N18V2B k obrazovaniyu

goryachikh treshchin pri svarke [The Effect of Boron on the Tendency of Heat-Resisting Type 1Kh13N18V2B Austenitic Steels to Form Hot Cracks on Welding], Svarochnoye proizvodstvo, No. 10, 1958.

17. A.Ye. Runov, F.I. Pashukanis and K.V. Lyubavskiy, Nekotoryye voprosy svarki litoy austenitnoy stali 1Kh20N12T-L [Certain Problems of the Welding of 1Kh20N12T-L Cast Austenitic Steel], Svarochnoye proizvodstvo, No. 8, 1958.
18. B.I. Medovar and V.A. Lutsyuk-Khudin, K voprosu o lokal'nom razrushenii svarnykh soyedineniy austenitnykh staley [The Problem of the Local Failure of Austenitic-Steel Welded Joints], Avtomaticheskaya svarka, No. 12, 1961.
19. B.Ye. Paton, B.I. Medovar and Yu.V. Latash, Elektroshlakovyy pereplav staley i splavov v mednom vodookhlazhdayemom kristallizatore [Molten-Slag Electric Remelting of Steels and Alloys in a Water-Cooled Copper Crystallizer], Avtomaticheskaya svarka, No. 11, 1958.
20. M. Imai, T. Nakayama, Ch. Kinasita and D. Khirata, Issledovaniye legirovannoy stali s vysokim soderzhaniyem bora, primenyayemoy v yadernykh reaktorakh [Investigation of Alloy Steel with High Boron Content Used in Nuclear Reactors], Tetsu to hagane [Journal of Iron and Steel Institute of Japan], 1959, 45, No. 9.
21. G.V. Samsonov and K.I. Portnoy, Splavy na osnove tugoplavkikh soyedineniy [Alloys Based on Refractory Compounds], Oborongiz [State Publishing House of the Defense Industry], 1961.
22. R. Nakagava and Ya. Otoguro, Vliyaniye azota i bora na svoystva austenitnoy nerzhaveyushchey stali 18 Cr-12 Ni [The Effect of Nitrogen and Boron on the Properties of Austenitic Stainless Steel 18 Cr-12 Ni], Tetsu to hagane [Journal of the Iron and

Steel Institute of Japan], 1960, 46, No. 10.

Submitted 4 January 1962

SPECIAL FEATURES OF ELECTRONIC HEATING IN WELDING

N.A. Ol'shanskiy

(Moscow Power Engineering Institute)

The essential nature of the heating process in electron-beam welding, which enables us to explain the special heating characteristics in welding of aluminum and its alloys, is theoretically substantiated. The sequence of events in joint formation in welding of large thicknesses is pointed out.

Recently, the effect of heating by electron bombardment has been used in various technological processes associated with thermal action upon the metal (smelting of metal, welding, heat treatment, drilling and milling). This has considerably broadened the field of application of the electron beam.

Welding with an electron beam is a progressive method by which we may successfully join refractory and chemically active metals and nonmetallic materials which are impossible to weld by other methods.

Welding with an electron beam may guarantee a number of advantages in fabricating designs from widely applied metals: the seam metal is refined considerably, deformation is reduced, the welding of seams is accomplished in places that are inaccessible to ordinary methods and so forth [1, 2, 3].

Broad prospects for the use of the electron beam in welding have been mapped out as a result of the many advantages of this method. Here, it is important to know the conditions and characteris-

tics of the heating and formation of the joints that are produced by an electron beam. The high specific energy density and electron velocities are the reasons for certain characteristics of heating with the electron beam.

Investigations of recent years have established that electrons which possess a certain energy can penetrate matter. The layer thickness of material on passage through which an electron completely loses its speed determines the path of the electron.

The paths of comparatively low-energy (10-82 kv) electrons in metals were carefully studied by B.Schonland [4]. According to Schonland, the electron path is expressed by the relationship

$$\delta = 2{,}1 \cdot 10^{-12} \frac{U^2}{\rho} \text{ [cm]}, \qquad (1)$$

where δ is the path in cm; U is the accelerating voltage in volts and ρ is the density of the material in g/cm^3.

Figure 1 shows a diagram of the theoretical paths of electrons in certain materials at higher voltages.

It follows from theoretical and experimental data that the length of the electron path in a material is a linear function of the energy at high accelerating voltages; in regions of lower energy, it is proportional to the square of the initial energy.

Calculations made on the basis of Formula (1) indicate that the electrons may penetrate to a depth of several tens and even hundreds of microns as a function of the accelerating voltage and the properties of the metal. The depth of electron penetration into metal is small, but on taking it into account, we may explain certain effects which are associated with the characteristics of electronic heating in welding.

It is also important to know the rate of energy loss by the elec-

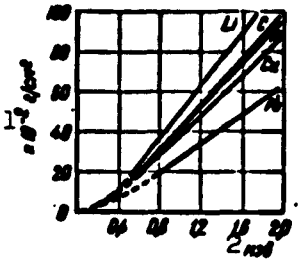

Fig. 1. Diagram of theoretical electron paths in lithium, carbon, aluminum, copper and lead. 1) X 10^{-2} g/cm^2; 2) Mev.

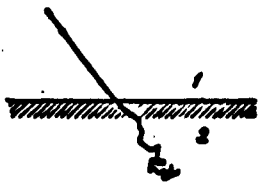

Fig. 2. Schematic representation of course of primary electron in material [11]. 1) Vacuum; 2) material.

tron over its path.

Study of absorption of a monochromatic electron flux [5, 6, 7] shows that an electron penetrating into a substance undergoes so-called multiple scattering and does not give up its energy immediately, but as a result of numerous collisions with the nuclei of the atoms and the electrons of the lattice. As a result of these collisions, the velocities and directions of the electrons which penetrate into the substance are changed.

As computations [8, 9] showed, the angle of probable deviation φ may be linked with the energy of electrons of atomic number $\underline{z}$ and with the thickness of the material $\underline{x}$ by the relation

$$\varphi = \frac{8\gamma}{\mu(\gamma^2-1)} - z\sqrt{1+\frac{1}{z}}\sqrt{\frac{\rho x}{A}}, \qquad (2)$$

where $\gamma = (E/\mu + 1)$, ρ is the density of the material, A is the atomic weight, $\underline{x}$ is the thickness of the material and $\mu = m_0V^2$ (where m_0 is the mass of the electron and V is its velocity).

It is apparent from this expression that the angle of probable deviation φ increases with increasing thickness of the material which

is traversed by an electron. The deviations increase rather sharply with decreasing electron velocity μ. Therefore, it follows that the path of an electron in a material is not rectilinear, but, as a result of collisions with the nuclei of the atoms and the electrons of the lattice, it assumes a tortuous zigzag form (Fig. 2).

The enlargement of the angle of deviation as the electron energy declines results in the electron's losing the major part of its energy on the terminal leg of the path. An important conclusion follows from this: an electron gives up kinetic energy irregularly in the direction of its path.

Thus, in contrast to the usual widely applied sources of heat, which effect heating by transmitting heat through the metal's surface, electronic heating is accomplished in the material itself; the most intensive liberation of heat is observed at a certain depth.

Certain characteristics of electron heating which is associated with the liberation of heat in a layer of material may be determined by analyzing the differential equation of heat conduction with the source of heat in the material itself:

$$\frac{\partial t(x,\tau)}{\partial \tau} = a\frac{\partial^2 t(x,\tau)}{\partial x^2} + \frac{1}{C\rho} W(x,\tau), \qquad (3)$$

where $\underline{t}$ is the temperature of the medium in degrees, $\underline{x}$ is the distance from the surface of the metal in mm, τ is the time in seconds, $a = \lambda/C\rho$ (where λ is the thermal-conductivity coefficient of the metal in cal/cm·sec°C, C is the heat capacity of the metal in cal/g°C, ρ is the density of the metal in g/cm^3) and $W(x, \tau)$ is the intensity of the source – the quantity of heat liberated in a unit time in a unit volume at a given point in the metal.

The change in the magnitude of an electron's energy loss, computed per unit length of its path, can be described in the form of

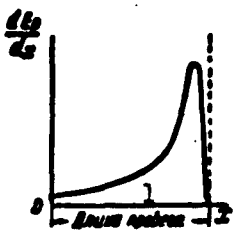

Fig. 3. Change in magnitude of energy loss as computed from unit length of path for primary electron along its path [11].
1) Length of path.

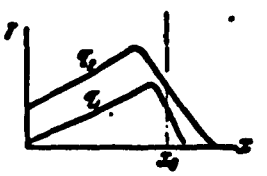

Fig. 4. Temperature change in layer of material with increase in impulse duration ($\tau_2 > \tau_1$) [12].

the curve reproduced in Fig. 3. It follows from the diagram that the magnitude of the energy loss by electrons has a maximum at a certain distance from the surface of the metal. On the basis of this curve, the quantity of energy liberated by an electron at a distance x from the surface may be approximated by the relationship

$$W(x) = -\frac{d(nE)}{dx} = C_0 e^{kx}, \qquad (4)$$

where n is the number of electrons passing through a unit cross section of the anode surface in 1 second, E is the average electron energy at a given point, C_0 is a constant and k is a coefficient which characterizes the absorption of energy in the metal.

Then, the differential equation of heating of the surface layer of the metal by the electron beam will take the following form:

$$\frac{\partial t(x,\tau)}{\partial \tau} = a\frac{\partial^2 t(x,\tau)}{\partial x^2} + \frac{C_0}{C_Q} e^{kx}. \qquad (5)$$

A similar problem has been solved by G.A. Titova [12], who investigated the effect of a high-power pulse discharge onto the anticathode metal of pulse tubes. Mathematical investigation of the solution of the equation shows that with increasing duration of the pulse, the layer of maximum temperature shifts toward the surface of the

metal as a result of heat conduction (Fig. 4) and that with a certain pulse duration, the maximum temperature will be on the surface of the metal.

The loss of a large quantity of electron energy under the surface of the metal in the pulsed heating regimes of electron beams explains the characteristics of the welding process of aluminum and its alloys.

It is known that the presence of refractory surface oxide films, the thickness of which reach 30 A [13], makes it hard to get good joints on such metals.

It has been established experimentally [14 and 15] that these metals may be welded with an electron beam only when it acts for brief periods – in the impulse regime. Coalescence of the edges does not take place on welding in a steady regime.

The positive effect of the pulse regime consists in the following: on welding, a large quantity of heat is liberated (almost instantly) in the inner layers of the metal under the surface layer of oxides as a result of which the internal layers melt instantly and are partially vaporized. This process acts like an explosion – the metal oxide films are destroyed and a high-quality welded joint is formed.

This proposition is confirmed by the work of Lange and Brach [6]. The authors were first to observe vaporization of the internal layer of metal under the influence of a high-power electron beam.

The distinctive characteristic of welding with an electron beam at high voltages is the possibility of obtaining a narrow, deep zone of penetration. In welding with an electron beam with a high specific energy density, the molten zone generally takes the form of an elongated cone with a seam-width-to-penetration ratio that approaches 10-15 (Fig. 5).

Figure 6 shows the microstructure of a penetration zone formed

with an electron beam; a distinct cast structure is evident. In the center of the molten zone, the grains are equiaxial and elongated toward the edges. The characteristic peculiarity of such penetration is the almost complete lack of a zone of thermal influence. The sharp transition from the molten to the base metal is apparent in the illustration.

The properties of the seam metal differ only slightly from those of the base metal; for example, the microhardness of the metal in the molten zone was 325 kgf/mm^2, while the hardness of the base metal was 332 kgf/mm^2.

Observation of the process and certain theoretical considerations give the following conception of electron-beam welding with deep penetration.

Welding with an electron beam that has a high specific energy density proceeds in the following manner. At the outset of the process, the area of the heated spot is equal to that of the beam's cross section. As a result of the liberation of a large quantity of heat in metal whose thickness is equal to the path of the electrons in the material, the metal in the heated spot vaporizes rapidly at the first moment of electron beam activity. As a result, a depression is formed in the shape of a cone whose lateral surface is larger than the base area by a factor of approximately e/R.

During formation of the conical depression, the specific beam energy density on the lateral face is decreased in approximately the same ratio. The angle at the peak of the cone is determined by the initial specific density of the energy in the beam and the thermophysical properties of the metal being welded (Fig. 7):

$$q = q_0 \sin \alpha; \qquad (6)$$

$$\sin\alpha = \frac{q}{q_0}, \qquad (7)$$

where q_0 is the specific power of the energy in the beam and q is the specific power of the energy on the lateral face of the penetration cone.

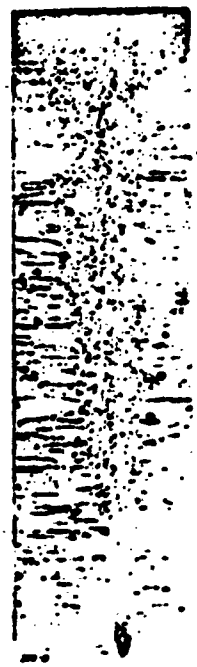

Fig. 5. Macrostructure of molten zone obtained in welding with high-energy electron beam on stainless steel (70X; reduced by half).

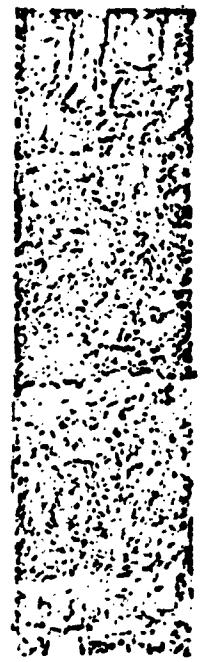

Fig. 6. Microstructure of penetration zone formed with electron beam (340X; reduced by half).

The specific energy density on the lateral face of the penetration cone, as computed from experimental data cited in a study based on the welding of zircalloy [17], is 25-30 watts/mm^2, while $\sin\alpha \approx$ ≈ 0.3.

The steady-state specific density of the energy on the lateral face of the cone of fusion should be of a magnitude such that intensive vaporization of the metal occurs.

The penetration cone is a stable formation, because when even part of it is filled with molten metal, the amount of energy absorbed by the surface increases sharply; this leads to boiling and vaporization of the metal from the filled portion of the cone and to restoration of its previous form.

Observations of the stable process of electron-beam welding show that melting of metal occurs on the front wall of the cone, after which the molten metal is displaced toward the rear wall of the cone, which is unheated by the electron beam (Fig. 8).

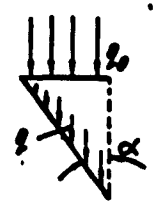

Fig. 7. Change of density of beam energy during formation of penetration cone.

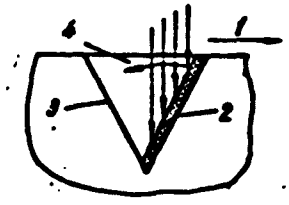

Fig. 8. Diagram of welding with deep fusion. 1) Direction of weld; 2) zone of vigorous heating with electron beam; 3) cooling and crystallization zone; 4) movement of molten metal.

The molten metal may be displaced from the electron beam's zone of influence into the crystallization zone under the pressure of the electron flux. In the welding process, the electron flux presses the molten metal with a force that may be computed from the formula [18]

$$p = nm_0V, \tag{8}$$

where m_0 is the mass of the electron at rest, V is the velocity of the electrons in the beam in m/sec, $\underline{n}$ is the number of electrons in the beam, and

$$n = \frac{I_a}{e_0} = \frac{q/U_a}{e_0}. \tag{9}$$

The velocity of an electron is determined by the expression

$$v = \sqrt{\frac{2e}{m_0} U_1}. \qquad (10)$$

where I_1 is the beam current in amp, q is the specific power in the spot in watts/mm^2, e is the charge of the electron in coulombs and U_1 is the accelerating voltage in volts.

Fig. 9. Emergence of electron beam at face of specimen (4X).

Proceeding from the values of (9) and (10), Formula (8) may be written

$$p = I_1 \sqrt{\frac{2m_0}{e} U_1}. \qquad (11)$$

It is apparent from this expression that the electron pressure is proportional to the beam current and to the square root of the accelerating voltage.

The absolute magnitude of the electron pressure is reckoned in tenths of a gram per square millimeter and is dependent upon the specific energy of the beam.

Thus, in the process of welding with an electron beam, the electron flux presses on the molten metal at the front wall of the penetration cone, while the metal at the rear wall does not experience this pressure. Therefore, as a result of the pressure difference, the molten metal is displaced from the heated zone into the zone of crystallization.

Figure 9 shows the point of exit of the electron beam on the butt of a specimen. It is apparent on the photograph that the beam melts a narrow zone in the metal from which the molten metal is displaced in the direction opposite to the pressure of the beam. The significant depression of the molten zone into the metal and the absence of a noticeable zone of thermal influence attest to the fact

that in beam welding, a sharper temperature gradient is observed than in arc welding. This contributes to an increase in the fraction of the heat expended on melting metal, improving the quality of the metal in welded joints, and increasing the technical-economic indices of the welding process.

REFERENCES

1. N.A. Ol'shankiy, Metod svarki elektronnym luchom v vakuume [Method of Welding with an Electron Beam in a Vacuum], Avtomaticheskaya svarka, No. 8, 1959.
2. N.A. Ol'shankiy and Yu.N. Zorin, Svarka metallov elektronnym luchom v vakuume [Metal Welding With Electron Beam in a Vacuum], Sbornik MVTU [Collection of the Moscow Higher Technical School (im. N.Ye. Bauman)], No. 101, Oborongiz [State Publishing House of the Defense Industry], 1961.
3. B.A. Movchan et al., Nekotoryye tekhnologicheskiye osobennosti svarki elektronnym luchom v vakuume [Certain Technological Features of Electron-Beam Welding in a Vacuum], Avtomaticheskaya svarka [Automatic Welding], No. 8, 1959.
4. B.F. Schonland, The Passage of Cathode Rays Through Matter, Proceedings of the Royal Society of London, Series A-Mathematical and Physical Sciences, London, Vol. 108, No. 745-748, May-August, 1925.
5. N. Bor, Prokhozhdeniye atomnykh chastits cherez veshchestvo [The Passage of Atomic Particles Through Matter], IL [Foreign Literature Publishing House], Moscow, 1950.
6. K. Sinel'nikov et al., Pogloshcheniye bystrykh elektronov v litii, uglerode, alyuminii, medi i svintse [The Absorption of Fast Electrons in Lithium, Carbon, Aluminum, Copper and Lead], ZhETF [Journal of Experimental and Theoretical Physics], Vol. 9, No. 2, 1939.
7. V.V. Gey and I.V. Piskunov, Rasseivaniye puchka bystrykh elektronov 1-2 mv [The Scattering of a Beam of Fast 1-2 mv Electrons], ZhETF, Vol. 9, No. 3, 1939.
8. W. Bothe, Durchgang von Elektronen durch Materie [Passage of

Electrons Through Matter], Handbuch der Physik [Handbook of Physics], XXIV/2, Berlin, 1933.

9. W. Bothe, Die Gueltigkeitsgrenzen des Gaussschen Fehlergesetzes fuer unabhaengige Elementarfehlerquellen [Limits of Validity of the Gaussian Error Law for Independent Error Sources], Zeitschrift fuer Physik [Journal of Physics], 4, 161, 1921.
10. S. Yu. Luk'yanov, O vtorichnoy elektronnoy emissii tverdykh tel [The Secondary Electron Emission of Solids], Izvestiya AN SSSR, Seriya fizicheskaya [Bulletin of the Acad. Sci. USSR, Physics Series], VIII, No. 6, 1944.
11. S.Yu. Luk'yanov, Fotoelementy [Photoelements], Izd. AN SSSR [Publishing House of the Acad. Sci. USSR], 1948.
12. G.A. Titova, Issledovaniye impul'snogo razryada pri nizkikh davleniyakh [The Investigation of Pulse Discharge at Low Pressures], Referat dissertatsii KFMN [Abstract of Dissertation KFMN (unlisted)], 1950.
13. N.A. Shishakov et al., Stroyeniye i mekhanizm obrazovaniya okisnykh plenok na metallakh [The Structure and Mechanism of Formation of Oxide Films on Metals], Izd. AN SSSR, 1959.
14. F. Lange and A. Brach, Strahlentherapie [Radiation Therapy], 50, 119, Munich-Berlin, 1935.
15. W.L. Wyman, High-Vacuum Electron Beam Fusion Welding, Welding and Metal Fabrication, No. 2, Vol. 37, 1958.
16. I.A. Stohr and I. Briola, Vacuum Welding of Metals, Welding and Metal Fabrication, No. 10, 1958.
17. G. Burton, Electron Beam Welding, Welding Journal, October, 1959.
18. K.H. Steigerwald, Schweissen und Schneiden mit Elektronenstrahlen [Welding and Cutting with Electron Beams], Schweissen und Schneiden [Welding and Cutting], No. 3, 1960.

Submitted 14 July 1961

INVESTIGATION OF DIFFUSION WELDING APPLICABLE TO ELECTROVACUUM APPARATUS

I.V. Afanas'yev and A.F. Khudyshev
(Moscow)

The operating conditions of electronic apparatus, which have recently come into widespread use, require high dependability of their welded joints both from the standpoints of static and dynamic strength and as regards the conductivity, high-temperature corrosion resistance and vacuum-tightness of the welded seam.

In the production of electrovacuum devices, such methods of joining components as arc welding in a protective medium, resistance roller welding, spot and projection welding and cold-pressure welding are used; the ultrasonic method and electron-beam welding in vacuo are also taking root.

A promising method of joining metals is diffusion welding [1]. At present, methods are being developed for obtaining vacuum-tight, high-temperature corrosion-resistant and vibration-resistant welded joints in the apparatus components by the use of diffusion welding in vacuo, where it is necessary to unite metals over a large contact surface with high finish and precision (0.02 to 0.05 mm); for joining components made of metals and alloys argon-shielded welding of which does not guarantee a vacuum-tight and high-temperature corrosion-resistant joint (titanium and MB copper, titanium and kovar, titanium and nickel and so forth); for producing a vacuum-tight, high-temperature corrosion-resistant and vibration-resistant metal-ceramic joint

in cerametallic assemblies (in place of soldering).

We should also note a number of positive qualities of diffusion welding in vacuo:

in the welding process, the vacuum heating of details proceeds under continuous evacuation; this makes it possible to remove the gases and oxide films from the parts to be welded before the squeezing force is applied to them;

the parts being welded are joined at a temperature equal to 60-80% of the melting point of the metal; this makes it possible to avoid warping of the parts and substantial changes in their properties in the weld-metal zone;

unlike metals may be united by this method;

the necessity of using gas envelopes, solders, electrodes, fluxes and so forth is dispensed with;

the application of a certain squeezing force to the parts being welded and the required assembly accuracy guarantee formation of welded units of high dimensional precision.

Equipment used for diffusion welding. Two semi-industrial plants have been designed and put in operation for experimental work to study the possibility of applying diffusion welding in the production of electronic apparatus and to develop a welding procedure for various metals used in electronics.

One of the installations (Fig. 1) enables us to weld components with diameters to 40 mm and lengths to 100 mm. The operating chamber consists of a quartz cylinder and a top cover and plate by means of which the chamber is hermetically sealed. The top cover has a side connection through which air is evacuated from the chamber. The plate has a bellows-and-rod assembly with which pressure is transmitted from the press to the component that we are welding. An inductor is situated

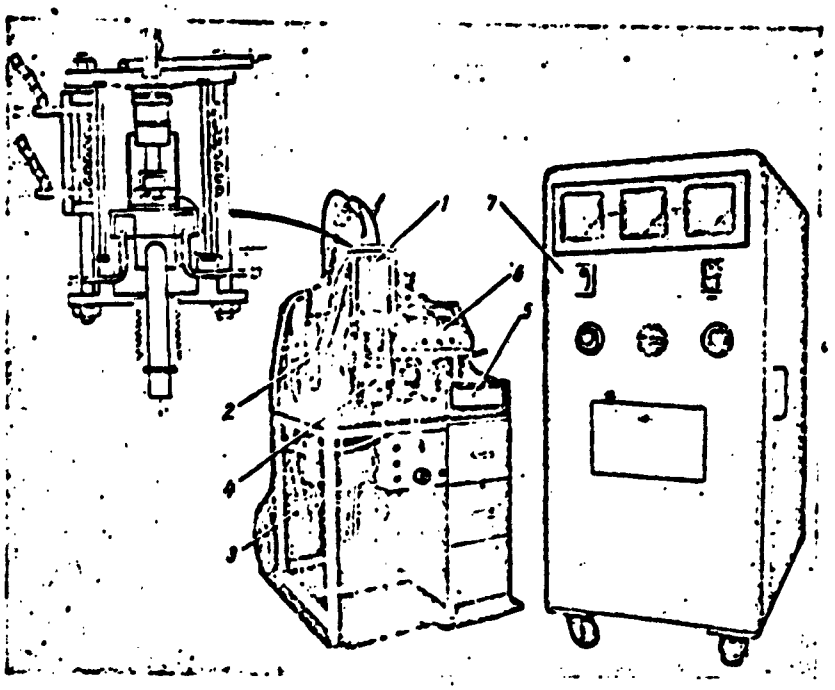

Fig. 1. Apparatus for diffusion welding of small parts in vacuo. 1) Vacuum chamber with volume of 1.7 dm^3; 2) type TsVL-100 oil-vapor pump; 3) type VN-461 mechanical pump; 4) 4-ton hydraulic press; 5) type MPShchPr-54 millivoltmeter for measuring temperatures to 1300^0; 6) type VIT-1 vacuum gauge; 7) type I060·012, 8-kw high-frequency generator.

outside the quartz cylinder. A thermocouple is inserted into the chamber to measure the heating temperature of the components. The pieces are cooled in the chamber by feeding water into the workholding mandrel.

Figure 2 shows the second apparatus for diffusion welding, which enables us to weld components with diameters to 150 mm and lengths to 200 mm. The operating vacuum chamber is a steel cylinder which is set up at the base of the press. There is an inspection hole in the front of the chamber; the lateral faces have windows with flanges to which are connected, on the left and right respectively, the vacuum system and the high-frequency coaxial input to the inductor which is placed inside the chamber.

The input (Fig. 3) is a coaxial design which provides vacuum-

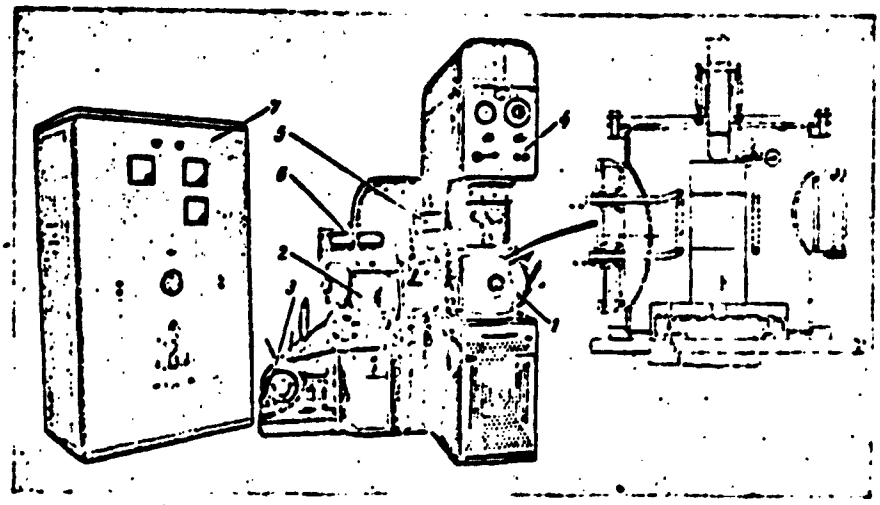

Fig. 2. Apparatus for diffusion welding of large parts. 1) Vacuum chamber with volume of 30 dm^3; 2) type VA-0.5-1 high-vacuum unit; 3) type VN-1 mechanical pump; 4) motor-operated 10-ton hydraulic press; 5) type MPShchPr-54 millivoltmeter for measuring temperatures to 1100°; 6) type VIT-1 vacuum gauge; 7) 20-kv high-frequency generator.

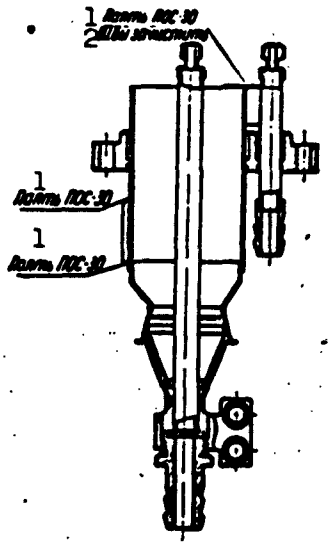

Fig. 3. Coaxial input. 1) POS-30 solder; 2) debur seam.

tightness, water cooling for the inductor, the high-frequency energy supply and insulation of the positive leadin terminal with respect to the grounded housing of the order of 5-7 kv.

The input consists of the following members. A socket with a tapered sleeve is soldered to a copper cylinder with a diameter of 80 mm. A ceramic insulator at the end of which is soldered a fitting of the copper supply pipe which terminates at one end in a connecting pipe for the water supply and on the other by a nipple for connecting the inductor is soldered to the tapered sleeve. A sleeve is soldered onto the connecting pipe

and fitted with a copper collar to connect the busbar of the high-frequency generator.

A steel flange with six holes for bolting the flange to the chamber by means of a copper packing spacer is soldered to the copper cylinder. A second supply line, which is terminated at one end by a nipple and at the other by a connecting pipe, is passed through the flange. It is possible to connect inductors with different diameters and numbers of turns to this input as a function of the dimensions of the components that we are welding.

The dimensions of the vacuum chamber permit the use of inductors with 3 to 12 turns and diameters to 140 mm. Therefore, components with diameters not more than 120 mm and [lengths] not greater than 200 mm may be welded in this chamber.

An energy concentrator made from MB copper with a certain internal surface configuration and water cooling is placed in the inductor. The surface configuration of the concentrator depends on the type of welded joint.

The chamber is closed at the top by the cover, which has a bellows assembly with a rod for transmission of pressure from the press slide onto the component that we are welding. The compressive force on the components being joined is measured by a dynamometer which is situated between the chamber rod and the press slide and enables us to determine the compressive force accurately within the range from 100-1000 kgf; forces greater than 1000 kgf are established and monitored with a manometer.

To reduce dissipation of heat into the chamber casing, the components to be welded must be set up on a ceramic base and ceramic disks laid over them.

The heating temperature of the welded components is measured with

the use of a thermocouple installed inside the press mandrel. The thermocouple is connected to a measuring device (millivoltmeter) through special ceramic inputs, which are connected, in turn, to the chamber by flanged joints with metallic packing spacers.

Certain working problems encountered in diffusion welding in vacuo. The essential problem in operation with apparatus for diffusion welding in vacuo is that of raising their efficiency. This is attained by "intensifying" the process, i.e., by reducing the duration of the preliminary and terminating operations, by accelerating the processes of evacuation, heating and subsequent cooling of the components, and by creating a semi-automatic multiposition system for diffusion welding.

The nature of the variation in the residual pressure in the operating chamber and the heating temperature in the diffusion welding process (Figs. 4 and 5) were investigated for this purpose.

It is apparent from Fig. 4 that 10-12 minutes are consumed in creating a high vacuum in the chamber. Then heating of the components leads to the inevitable liberation of gases adsorbed in them, the quantity of which is dependent upon the composition of the metal and the dimensions of the components that we are joining. The liberation rate of gases is dependent upon the heating rate. Here the pressure in the chamber is increased (line bc). The segment cd characterizes the steady pressure in the chamber during the evacuation of the gases. This process may be accelerated by increasing the heating temperature, using a more powerful pumping system. Otherwise, the pressure increase to 10^{-3} mm Hg may cause ionization of the gases and sparkover (short-circuiting between the coils of the inductor). After evacuation of the gases, the residual pressure in the chamber is reduced to 10^{-4} mm Hg (line de), after which the necessary squeezing force is applied to the pieces.

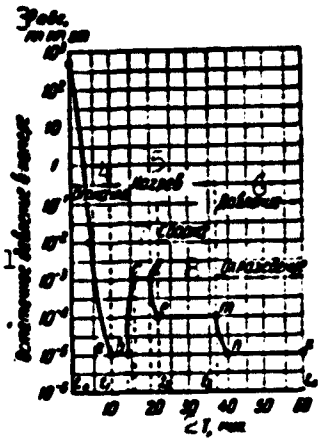

Fig. 4. Curve of residual pressure variation in diffusion welding of metals. 1) Residual pressure in chamber; 2) T, minutes; 3) P_{abs}, mm Hg; 4) evacuation; 5) heating; 6) pressure; 7) welding; 8) cooling.

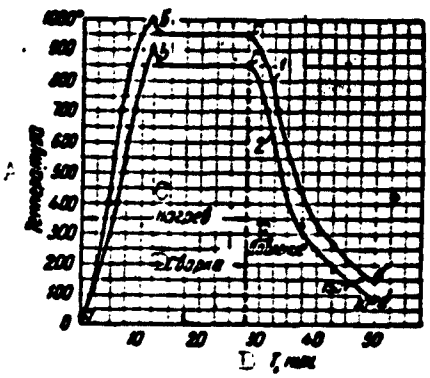

Fig. 5. Curve of temperature variation in diffusion welding of metals. 1) Kovar; 2) copper. A) Temperature; B) T, minutes; C) heating; D) welding; E) pressure.

The segment em of the curve characterizes a direct welding process with a duration of 15-20 minutes. When this time has elapsed, heating is discontinued and the pressure of the residual gases drops in the chamber.

The squeezing force is not removed until the components cool to a temperature of 80-150°. In the case of welding of unlike metals, a premature pressure drop leads to rupture along the butt-joint line, and when welding like metals, the ultimate strength of the welded seam is reduced.

The curve of the residual pressure variation in the working chamber was recorded in welding components of oxygen-free copper and the character of the curve was retained when components of other metals were welded.

It is apparent from Fig. 5, which was obtained in welding compo-

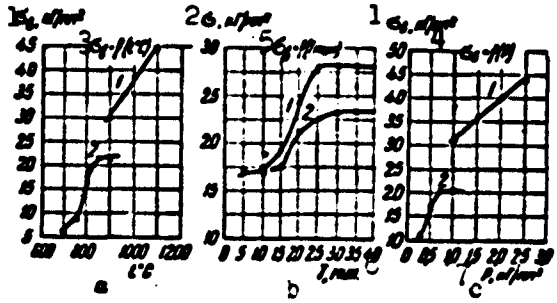

Fig. 6. Dependence of welded-joint strength upon fundamental parameters of diffusion welding of kovar to kovar (1) and MB copper to MB copper (2). a) P = 2.0 kgf/mm^2 = const, T = 20 minutes = = const (1); P = 0.7 kgf/mm^2 = = const, T = 20 minutes = const (2); b) t = 1000° = const, P = = 1.0 kgf/mm^2 = const (1); t = = 850° = const, P = 0.7 kgf/mm^2 = = const (2); c) t = 1000° = const, T = 15 minutes = const (1); t = = 850° = const, T = 20 minutes = const (2). 1) σ_b, kgf/mm^2; 2) σ, kgf/mm^2; 3) $\sigma_b = f(t°C)$; 4) σ_b = = f(P); 5) σ_b = f(T minutes); 6) T, minutes; 7) P, kgf/mm^2.

nents made of MB copper and kovar, that to heat to the optimum temperature, at which welding takes place, it is necessary first to raise the temperature somewhat above optimum (by 50-70°), since on application of pressure to the components that we are welding, some of the heat is driven, due to enlargement of the contact, into the pressing apparatus and is partially expended on diffusion of particles of one metal into the other.

After completion of heating, the objects being welded should be cooled to a specified temperature which should not exceed 150° for components composed of ferrous metals and 80° for nonferrous metals to avoid oxidation in air.

Certain results of investigation of vacuum diffusion welding procedure with metals employed in electrovacuum production. To finalize a procedure for vacuum diffusion welding of the metals and alloys which are employed most frequently in the preparation of electrovacuum apparatus, we studied the dependence of the strength, vacuum-tightness and high-temperature corrosion resistance of the welded joint upon the fundamental parameters of the process, i.e., the specific pressure P (kgf/mm^2), the heating temperature t ($^{\circ}C$) and the heating time T (minutes) in welding of certain metals (copper, kovar, nickel, steel 10, titanium and others).

As an example, Fig. 6 shows the dependence of the strength of the welded joint upon the fundamental parameters of diffusion welding for copper and kovar. The optimum welding conditions are given in the table.

1 Свариваемые металлы	2 t, град	3 P, кГ/мм²	4 T, мин.
5 Медь МБ с медью МБ	800÷850	0,5÷0,7	15÷20
6 Ковар с ковром	1000÷1100	1,5÷2,0	20÷25

1) Metals welded; 2) t, degrees; 3) P, kgf/mm^2; 4) T, minutes; 5) MB copper; 6) kovar to kovar.

It was established that essential influence on the quality of joints formed by diffusion welding is exerted by the machining finish and preparation of the surface of the components. Good results were obtained when the surface was machined with a lathe tool to a finish of not less than ∇7 with subsequent annealing in a hydrogen medium. When the components were ground, the strength of the joint was reduced by 15-20%; this apparently is explained by working of abrasive particles into the surfaces of the objects.

It is necessary to subject the components to surface etching

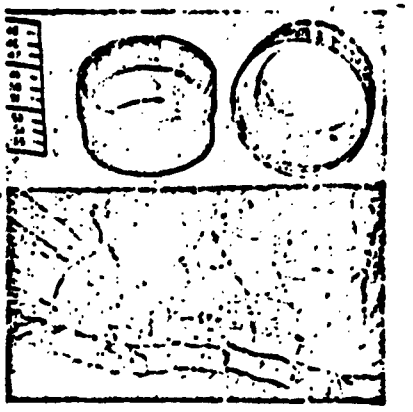

Fig. 7. General appearance of unit and microsection of joint between MB copper and aluminum foil.

prior to welding, with subsequent rinsing with alcohol or chemically pure acetone.

Experiments were conducted with hydrogen admitted into the chamber when welding apparatus units from copper plates. The components to be welded were heated to 800°, the chamber filled with purified hydrogen and the hydrogen evacuated over a period of 10-20 minutes, after which welding was performed. The hydrogen contributed to reduction of the oxides on the surfaces of the components to be welded.

Figure 7 shows the general appearance and microsection of the welded joint of a cup made from MB copper 1.5 mm thick with aluminum foil 0.018 mm thick. The joint was vacuum-tight and strong when welded under the following conditions: t = 520°, P = 1.0 kgf/mm^2 and T = 10 minutes.

Metallographic investigations showed that two diffusion layers formed between the metals that were being welded: the first, with a thickness of 2-4 μ, which adjoined the aluminum foil, was rich in copper and had a fine-disperse structure – a eutectic; the second layer, 4-16 μ in thickness, which adjoined the copper, was a solid solution of aluminum in copper – an α-solid solution.

A procedure of vacuum diffusion welding of ferrous metals was also developed; Armco iron to Steel 10, Steel 45 to KhVG steel, Steel 3 to Steel 10, molybdenum to EI437B alloy, VT3 titanium to 1Kh18N9T and other metals. At present, a welding procedure is being elaborated for unlike nonferrous metals, whose joints are currently impossible to produce with other welding and soldering methods.

An important problem is the creation of an improved semiautomatic industrial system with programmed control for diffusion welding of metallic and cerametallic electrovacuum apparatus in vacuo.

CONCLUSIONS

1. Two semi-industrial installations were built for vacuum diffusion welding of metals and ceramics to metal.

2. A procedure was developed for diffusion welding of certain metals employed in the design of electrovacuum apparatus.

3. The dependence of the strength, vacuum-tightness and high-temperature corrosion resistance of welded joints upon the fundamental parameters of diffusion welding for MB copper, kovar and other metals was investigated.

Manuscript Page No.

[List of Transliterated Symbols]

35 л = l = luch = beam

44 абс = abs = absolyutnyy = absolute

REFERENCES

1. N.F. Kazakov, Svarka davleniyem v vakuume raznorodnykh metallov [Pressure Welding of Various Types of Metals in Vacuum], Svarochnoye proizvodstvo [Welding Practice], No. 8, 1958.
2. R. Berrer, Diffuziya v tverdykh telakh [Diffusion in Solids], IL [Foreign Literature Publishing House], Moscow, 1948.
3. L.M. Mirskiy, Protsessy diffuzii v splavakh [Diffusion Processes in Alloys], Oborongiz [State Publishing House of the Defense Industry], 1959.
4. M.G. Lozinskiy, Vysokotemperaturnaya metallografiya [High-Temperature Metallography], Mashgiz [State Scientific and Technical Publishing House of Literature on Machinery], 1956.
5. S.D. Gertsriken and I.Ya. Dekhtyar, Diffuziya v metallakh i splavakh v tverdoy faze [Diffusion in Metals and Alloys in the Solid Phase], Fizmatgiz [State Press for Physicomathematical Literature], 1960.
6. A.P. Semenov, Skhvatyvaniye metallov [Seizure of Metals], Mashgiz, 1958.

Submitted 24 June 1961

MOLTEN-SLAG ARCLESS ELECTRIC WELDING OF VT5-1 TITANIUM ALLOY

S.M. Gurevich and V.P Didkovskiy

(Order of the Red Banner of Labor Electric Welding Institute imeni Ye.O. Paton, Acad. Sci. UkrSSR)

N.N. Tikhov

(Moscow)

The formable VT5-1 titanium alloy belongs to the titanium-aluminum-tin system. At normal temperature, the alloy is single-phased (α-phase) as a result of which it welds satisfactorily. As compared with other titanium alloys, particularly those alloyed with β-stabilizing elements, the VT5-1 alloy possesses elevated strength under long-term loading at temperatures to 500° and under shock heating to 900°.

The high-temperature strength of the type of alloy under consideration is considerably improved as a result of complex alloying of the titanium with aluminum and tin [1, 2]. The VT5-1 type alloy, owing to its satisfactory weldability, is widely used in the production of welded thin-sheet designs.

Significant interest is attracted to the feasibility of welding large-section details made of this alloy. A positive solution of this problem would make it possible to broaden the field of application of the alloy.

In the present paper, the results of investigations made on the introduction of molten-slag arcless electric welding to series pro-

duction of objects made from the VT5-1 titanium alloy are cited.

The study was conducted in two directions: welded joints made from forged pieces and extruded profiles were investigated. In fabrication of components of comparatively small section (approximately 60 X 60 mm), the use of pressed blanks is extremely promising. The welding was conducted with plate electrodes on an A-550 apparatus; power from a single-phase TShS-3000-1 transformer had a "hard" characteristic [3]. AN-T2 flux was used and the slag pool was shielded with pure Composition One argon.

Welding of forged pieces. The chemical composition and mechanical properties of the VT5-1 alloy are assembled in Table 1. The certificate characteristics of the alloy also appear in this table.

TABLE 1

1 Металл	Содержание элементов, % вес. Al	Sn	3 $\sigma_в$, кГ/мм²	δ, %	ψ, %	4 $a_н$, кГ·м/см²
Поковка 5 60×60 мм . .	4,52	2,52	88,2—90,4 / 89,3	10,4—11,2 / 10,8	24,8—30,6 / 27,8	5,6—6,1 / 5,8
Пластинчатый 6 электрод 12×60 мм . .	4,20	2,10	80,9—82,3 / 81,6	10,7—15,0 / 11,1	24,6—30,6 / 27,6	5,8—6,4 / 6,1
Сплав ВТ5-1, 7 паспортные данные	4—5,5	2—3	75—95	8—12	25—40	4—9

1) Metal; 2) element content, % by weight; 3) σ_b, kgf/mm^2; 4) a_n, kg·m/cm^2; 5) 60 X 60 mm forged piece; 6) 12 X 60 mm plate electrode; 7) VT5-1 alloy, certificate data.

The following optimum conditions were selected for welding forged pieces: I_{sv} = 1600 to 1800 amp, U_d = 14 to 16 volts, the argon feed for protection of the slag bath was 8.0 liters/min, the gap between the edges of the pieces that were being welded was 26 mm and the weight of the flux supplied was 130 g. The above regime guaranteed a full and rather uniform penetration of the edges, sta-

bility of the molten-slag arcless electric process and good joint shaping.

Figure 1 shows the macrostructure of a welded joint of forgings of the VT5-1 alloy, which was produced by the molten-slag arcless electric method, while Fig. 2 shows its microstructure.

Fig. 1. Macrostructure of welded joint produced between forgings of VT5-1 titanium alloy, by molten-slag arcless electric method. Etching with reagent of following composition: 30% HF, 30% HNO_3, 40% H_2O.

It is apparent from the photographs shown that the macrocrystalline structure usually observed with molten-slag arcless electric welding is characteristic of the seam metal. The acicular structure of the seam metal and around-the-weld zone, as well as the forged base metal, signifies a $\beta \rightarrow \alpha'$ martensite transformation on cooling.

As we know, in the presence of these structures, it is particularly important to provide reliable protection for the titanium alloy that we are heating to high temperatures from contamination by harmful gaseous admixtures (nitrogen, oxygen and hydrogen). Only under this condition may we obtain high plasticity and toughness in the metal. The results of the investigations show that molten-slag arcless electric welding using the oxygen-free AN-T2 fluoride flux and argon shielding fully satisfies these requirements. As an example, the impurity content in a metal seam between forgings with a 60 X 60 mm section is given in Table 2. For comparison, the results of analysis of the base metal are given in the same table.

The nitrogen concentration was determined chemically, the oxygen and hydrogen concentrations by the method of vacuum melting in

Fig. 2. Microstructure of different sections of welded joint between VT5-1 titanium alloy forgings (300X). a) Base metal; b) seam metal; c) around-the-weld zone.

TABLE 2.

1 Металл	2 Содержание примесей, % вес.					
	N_2	O_2	H_2	C	Si	Fe
Шов . . 3	0,038	0,03	0,008	0,23	0,08	0,10
Основной .4	0,050	0,03	0,008	0,20	0,09	0,08
Пластинчатый электрод 5	0,036	0,026	0,006	0,22	0,06	0,10

1) Metal; 2) impurity content, % by weight; 3) seam; 4) base; 5) plate electrode.

an apparatus used for gas analysis, and the carbon, silicon and iron concentrations by the spectral method.

It follows from the table that the impurity content, including that of the gases, is practically the same in the seam metal and in the original metal. The hardness curves of the different structural portions of the welded joint (Fig. 3) also attest to the absence of additional seam contamination by harmful admixtures in the welding process. As we see from the diagram, the hardness of the seam does not differ from those of the base metal and around-the-weld zone.

Cracks, pores and other defects were absent in the welded joints. Test results for the mechanical properties of welded seams (Table 3)

TABLE 3

1 Термическая обработка	2 $\sigma_в$, кг/мм²	δ, %	ψ, %	3 $a_н$, кг·м/см² 4 металл шва	5 околошовная зона
6 Без термообработки	80.2—85.5 / 83.6	8.1—9.2 / 8.6	19.1—22.0 / 21.0	5.1—6.0 / 5.5	5.5—5.8 / 5.7
7 Отжиг при 800°	81.4—86.1 / 84.1	7.9—10.0 / 8.4	19.6—23.0 / 21.8	4.9—5.9 / 5.4	5.6—5.9 / 5.8

1) Heat treatment; 2) σ_b, kg/mm^2; 3) a_n, kg·m/cm^2; 4) seam metal; 5) around-the-weld zone; 6) without heat treatment; 7) annealing at 800°.

showed that the joints were equally as strong as the base metal and had satisfactory plasticity and toughness.

Annealing at 800° produced no noticeable change in the mechanical properties of the welded seam. The same phenomenon is observed in an α-alloy based on titanium, whose strength, plasticity and toughness change negligibly after heat treatment below the critical temperature region of the $\alpha \rightarrow \beta$ transformation.

The investigations carried out enabled us to conclude satisfactory weldability of the VT5-1 titanium alloy in large thicknesses; this is confirmed in series production of welded articles with thicknesses to 70 mm.

Welding of extruded sections. The joint between blanks with rectilinear sections from 40 X 42 to 55 X 64 mm was taken as an example of molten-slag arcless electric welding of extruded sections prepared from the VT5-1 alloy. The blanks were welded under the following conditions: I_{sv} = 1400-1800 amp, U = 13.8-17 volts, argon feed for the protection of the slag bath 6-8 liters/min, and electrode formed by a plate 8 mm in thickness.

Figure 4 shows a joint welded between extruded blanks with a 42 X 47 mm section, by the molten-slag arcless electric method.

The results of the investigations showed that the quality of the

extruded sections was inconsistent. Together with rather high plasticity and toughness indices (δ = 12-13%, a_n = 5kg·m/cm^2 and greater), blanks having δ < 7% and a_n < 3 kg·m/cm^2 were encountered.

As a result of this, the application of extruded strips (forged or milled to a thickness of 8 mm) as plate electrodes failed to produce positive results. As mechanical-property tests on the welded joints* showed, the seam metal in this case possessed an extremely high strength which exceeded 100 kgf/mm^2, with low plasticity and impact strength (the elongation per unit length was reduced to 4-5% and the impact strength to 1.5 kgf·m/cm^2). This was indicative of the elevated content of gas admixture in the original metal – the extruded blanks and plate electrodes.

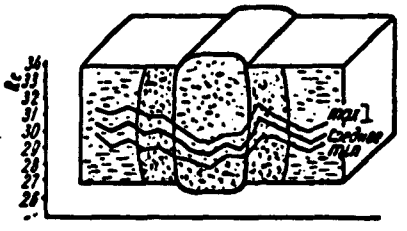

Fig. 3. Hardness of seam welded between forged pieces by molten-slag arcless electric method; butt joint. 1) Average.

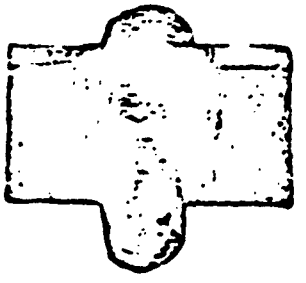

Fig. 4. Welded joint between extruded blanks.

The plasticity of the seam metal increased considerably as a result of using plate electrodes made from unalloyed commercial type VTI-1 titanium. It is apparent from Table 4 that a seam welded with such an electrode possesses reduced strength with a higher plasticity than when welded with an alloyed electrode.

In the case of welding with an unalloyed titanium electrode, however, we also failed to avoid a change in the plasticity of the seam metal as a result of instability in the composition and properties of the base metal. Thus, for example, when 42 standard specimens with a

TABLE 4

1	2		3	
[illegible]	σ_b, kgf/mm²	δ, %	ψ, %	a_n, kgf·m/cm²
43×56	62.2—62.5 / 62.3	13.4—15.2 / 14.6	24.8—29.8 / 27.4	3.9—5.1 / 4.3
47×61	64.0—65.3 / 64.5	19.2—20.8 / 20.0	35.2—46.2 / 41.8	4.05—4.15 / 4.1
55×64	61.0—61.2 / 61.1	12.0—17.2 / 15.8	35.4—37.4 / 36.2	4.15—4.75 / 4.5

1) Blank section, mm; 2) σ_b, kg/mm²; 3) a_n, kg·m/cm².

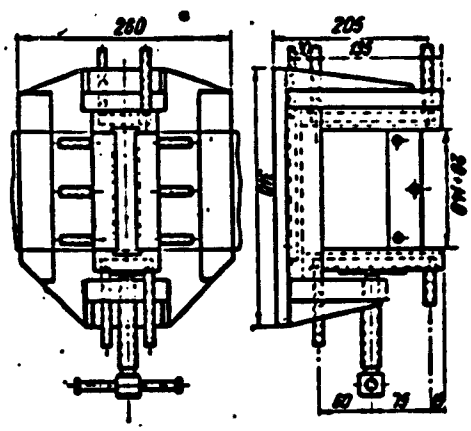

Fig. 5. Copper chill mold for molten-slag arcless electric seam welding.

notch on the axis of the seam that had been cut from joints between extruded sections of different lots were tested for impact bending, the following results were obtained: 15 specimens had impact strengths below 3 kgf·m/cm², 25 specimens from 3 to 5 kgf·m/cm² and two specimens had impact strengths above 5 kgf·m/cm². The mechanical properties of the base metal also varied in the same manner.

Thus, by using an unalloyed filler metal in molten-slag arcless electric welding on the VT5-1 titanium alloy, it is impossible to ob-

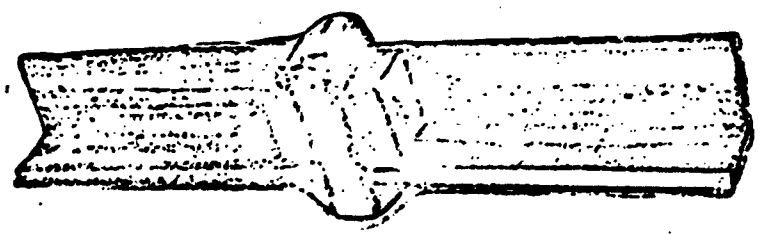

Fig. 6. Welded joint between extruded sections, with inserts.

tain a joint equal in strength to the base metal. In such a procedure, the use of which may be regarded only as a forced measure of eliminating the brittle properties of welded seams where the plasticity of

the base metal is reduced, the strength of the seam metal is reduced by 15-20% as compared with the base metal. Occasionally, this reduction in the strength of the welded joint is permissible. Nevertheless, equal strength of the welded joints and base metal is highly desirable. This may also be attained with a joint between components prepared from pressed sections by increasing their quality and property stability. In this case, we may use an electrode of the same composition as that of the base metal and avoid a decrease in strength while retaining sufficient plasticity of the seam metal.

Industrial use of molten-slag arcless electric welding of rings from VT5-1 alloy. Rings of various diameters were assembled from two halves of forged or forge-rolled extruded blanks with sections to 60 X X 70 mm. This process was accomplished on a turntable in two water-cooled copper molds (Fig. 5). The blowdown of argon from the baffle plates above the slag bath is well executed in this design. To fit the blanks tightly to the walls of the mold, the faces of the half-rings are machined over a length of 30-40 mm to a rectangular section on a milling machine. In welding angle-stock or other extruded sections, the sections are reduced to rectangular shape with the use of inserts made from an alloy of similar composition (Fig. 6) to prepare the components for welding. The general appearance of the welding apparatus and table with a ring mounted on it is shown in Fig. 7.

An automatic welding procedure developed for the rings guarantees high process efficiency. The welding time for a single joint does not exceed 4-5 minutes.

The welded ring joints are quality-controlled by x-ray beams. Tight seams are obtained without defects. Nor can defects be detected in the seams after the rings are machined.

An AN-T2 flux which is melted down in graphite crucibles with a

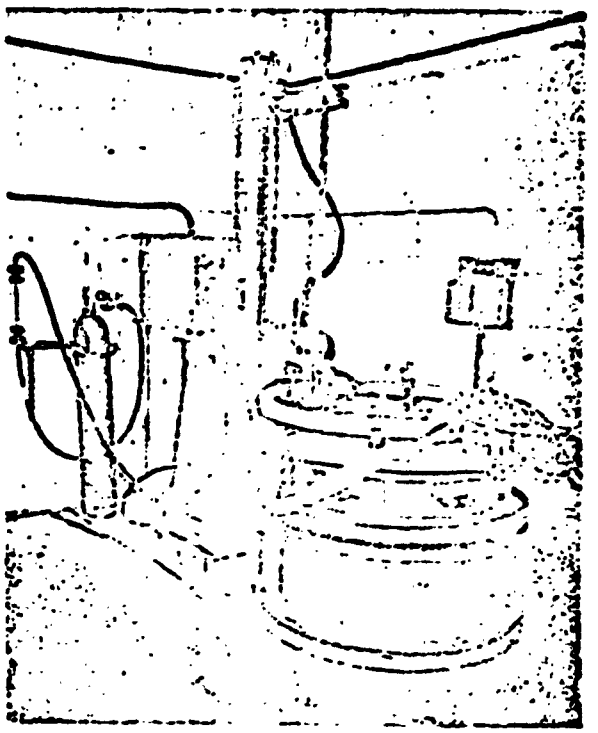

Fig. 7. General appearance of apparatus with turntable for molten-slag arcless electric welding of rings.

high-frequency apparatus is employed in series production. Immediately before welding, the flux is roasted for 1.5-2 hours at a temperature of 250-300°.

CONCLUSIONS

1. Large-section components prepared from the VT5-1 titanium alloy can be welded successfully by the molten-slag arcless electric welding method, using AN-T2 flux.

2. In welding forged pieces with plate electrodes prepared from the VT5-1 alloy, the welded joints are equally as strong as those of the base metal, with satisfactory plasticity and toughness of the joints.

3. For the purpose of improving the quality of welded joints prepared from extruded sections of VT5-1 alloy, it is necessary to in-

crease the plasticity and toughness of the blanks.

4. Molten-slag arcless electric welding of different size rings from the VT5-1 titanium alloy was introduced into batch production.

REFERENCES

1. A.D. Makkvillen and M.K. Makkvillen, Titan [Titanium], Metallurgizdat [State Scientific and Technical Publishing House for Literature on Ferrous and Nonferrous Metallurgy], 1958.
2. I.W. Suiter, Tensile Properties of Some Titanium Ternary Solid Solutions and Duplex Alloys up to 600°C, Journal of Institute of Metals, Vol. 84, No. 10, 1955.
3. S.M. Gurevich, V.P. Didkovskiy et al., Avtomaticheskaya dugovaya i elektroshlakovaya svarka v proizvodstve izdeliy iz titana sredney i bol'shoy tol'shchiny [Automatic Arc and Molten-Slag Arcless Electric Welding in the Production of Articles of Medium and Large Thickness from Titanium], Collection entitled Vnedreniye novykh sposobov svarki v promyshlennost' [The Introduction of New Welding Methods in Industry], Kiev, 1960.

Submitted 23 May 1961

Manuscript Page No.	[Footnote]
54	The tests were conducted by L.S. Solov'yeva.

Manuscript Page No.	[List of Transliterated Symbols]
50	св = sv = svarka = welding
50	д = d = duga = arc

PRESS WELDING OF ROLLED SECTIONS OF ALUMINUM-MAGNESIUM ALLOYS

A.I. Shestakov and A.A. Rossoshinskiy

(Institute of Electrical Engineering of the Acad. Sci. USSR)

A procedure for press welding rolled sections of type AMg aluminum-magnesium alloys with sections of 6000 mm^2 and greater has been developed and introduced to industry by the Institute of Electrical Engineering of the Academy of Sciences of the USSR jointly with machine-building concerns under the direction of Academician K.K. Khrenova of the Academy of Sciences of the USSR. To our knowledge, there has been no information relating to press welding of details of this section published in the domestic and foreign literature.

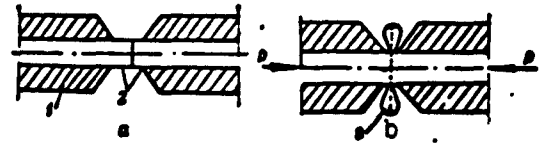

Fig. 1. Diagram of press welding. a) Initial welding period; b) final welding period. 1) Gripping device; 2) components to be welded; 3) flash.

Vast experimental and theoretical investigations which were conducted both in laboratories and under industrial conditions preceded development of the procedure. A procedure for butt welding rectangular sections was developed and introduced in 1960 and laboratory experiments which produced positive results were conducted on the basis of butt welding of a section with a developed shape.

A diagram of the press welding process is shown in Fig. 1. The

components to be welded are placed in special gripping devices, heated to the temperature at which the given metal becomes soft, and squeezed together. Under the influence of the force P, the metal in the zone of the butt joint flows plastically, the surfaces that we are joining are drawn together to a distance which is comparable to the dimensions of atomic radii, the interatomic bonding forces come into play and a monolithic joint is formed. The surface films, impurities and inclusions which inhibit the work of the interatomic bonds are forced out into a flash. We should take into consideration that the press welding process is accompanied by diffusion and recrystallization as a result of heating.

The scheme of press welding is simple; however, when developing a welding procedure for various alloys and components, it was necessary to solve a series of problems, including the following: to find the optimum heating temperatures of the components to be welded and to determine the quality and method of preparation, the squeezing force, the overhang of the components and so forth, not to mention the design of the jigs for press welding.

Laboratory investigations and practical experiments showed that the optimum heating temperature of components for press welding is dependent upon the chemical composition of the alloy and lies within a range which somewhat exceeds the critical points Ac_3. To prevent undercooling in the components during the time required to transfer them from the furnace, fasten them in the gripping devices, clean the surfaces and so forth, the actual heating prior to welding should be 20-35% higher. Moreover, to prevent overheating, we are also prohibited from subjecting the metal to excessive heating. Table 1 gives the optimum heating temperatures of certain aluminum-magnesium alloys and the specific pressures on welding.

TABLE 1

1 Сплав	2 Температура нагрева, °С	3 Осадка
АМг3 4	400—430	80% осадки, что соответствует удельному давлению ~150кГ/мм² 7
АМг5ВМ 5	430—450	
АМг6 6	450—480	

1) Alloy; 2) heating temperature, degrees; 3) upsetting; 4) AMg3; 5) AMg5VM; 6) AMg6; 7) 80% upsetting; this corresponds to a specific pressure ~150 kgf/mm^2.

Subsequent to heating, the surfaces that are to be butted should be cleaned with a degreased wire brush (wire thickness 0.2-0.3 mm). In addition to this, we should also clean the lateral faces which project from the grips.

The length of the projecting ends of the components to be welded is selected so that the area of the surfaces that are being welded is doubled on full upsetting. In this case, according to the stability conditions of the process, the length of the profile overhangs should be minimal, and upsetting carried out in several stages. This is extremely important in order that the lateral faces are not deformed by the gripping devices in the welding process. For this reason, the surfaces of the gripping devices must be developed so that in the welding process, the component will be restrained by friction.

Figure 2 shows a specimen of a joint made in aluminum-magnesium alloy that was welded at the butt; Fig. 3 shows the macrosection of this joint. There are no defects in the zone of the butt weld; a line of demarcation is indiscernable. The results of mechanical tests on joints produced by press welding are assembled in Table 2; data relating to the base metal are also assembled in the same table.

The bending angle of specimens cut from the seam was somewhat smaller than that of specimens cut from the base metal. The latter, however, is explained by the fact that the direction of the fiber in a welded butt joint coincides with the direction of the force applied to bend the specimens. As we know, the aluminum-magnesium alloys possess significant anisotropy of properties. The strength of the

TABLE 2

1 Образцы	2 $\sigma_в$, кгс/мм²	3 α, град	4 Примечание
5 Основной металл АМг3	20,0—22,6 / 21,6	180—180 / 180	
6 АМг5В	27,5—30,1 / 28,3	120—160 / 150	9 Разрыв по основному металлу
7 Участок сварки АМг3	19,5—25,5 / 21,0	102—180 / 160,5	
8 АМг5В	26,0—30,0 / 28,1	80—140 / 120	

1) Specimen; 2) σ_b, kgf/mm^2; 3) α, degrees; 4) remarks; 5) AMg3 base metal; 6) AMg5B; 7) welding section of AMg3; 8) AMg5V; 9) break through base metal.

metal is greater in the direction of the grain than it is across the grain.

The impact strength of specimens taken from a section of a butt joint was 50% lower than that of the base metal and was 2-2.5 kgf·m/cm^2 on the average for the AMg3 alloy. This may be explained by the same factors which influence the bending angle. The latter is confirmed by the fact that the bending angles and impact strengths of specimens cut from the base metal perpendicular to the texture of the rolled stock did not differ from the same properties of the specimens cut from the zone of the butt joint. In all cases, the specimen strengths of the joints

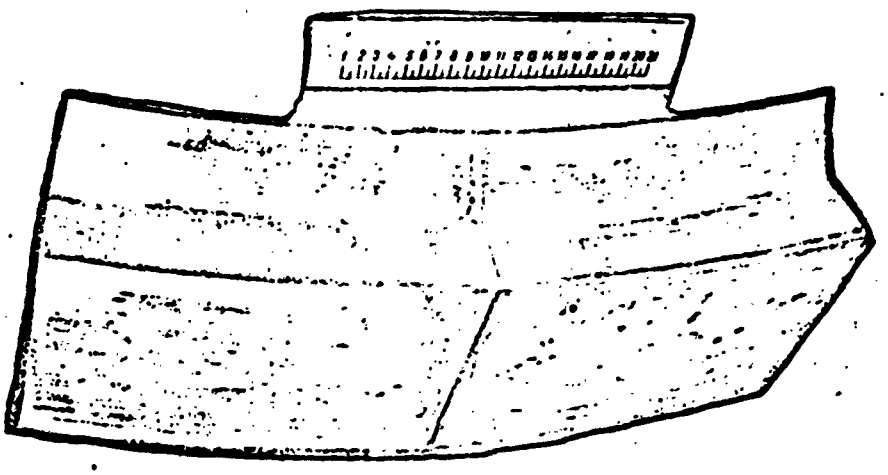

Fig. 2. Joint produced by press welding at butt of shaped rolled section of aluminum magnesium alloy.

formed by press welding were 10-15% above those of seams formed manually by argon-shielded welding even though the plasticities and impact strengths were the same.

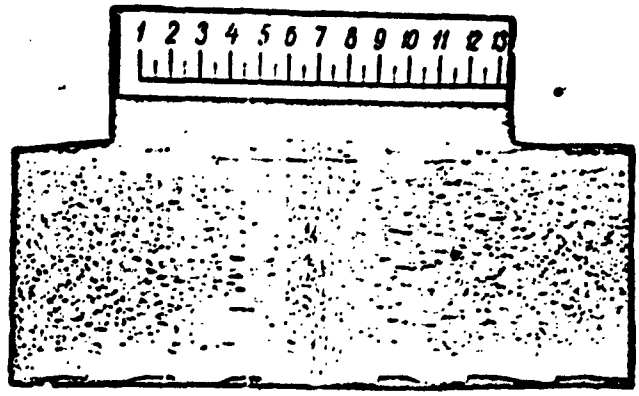

Fig. 3. Macrostructure of joint produced by press welding at butt.

Metallographic investigations showed that the metal structure in the zone of a joint produced by press welding is fine-grained; there is no superheated zone. The structure in the zone of the butt joint, as a rule, is double-phase and consists basically of a solid-solution phase (magnesium in aluminum) and an insignificant quantity of the β-phase. The hardness of the metal in the seam zone was 10% above that of the base metal.

The high plasticity and strength of a welded joint, in spite of the fact that the metal in the welding zone is subjected to considerable plastic deformation, may be explained by various factors. Thus, we should assume that at the initial moment of welding, when the metal flows freely, a considerable number of dislocations form. Accumulations of vacancies which may act as embryonic macrocracks appear at the intersections of the dislocations and their concentrations, which form subboundaries. Therefore, if the welding process is terminated before the free flow of metal is discontinued in the zone of the butt joint, a large number of fine-structure defects will be retained in the welding zone, and this will reduce the mechanical properties of the welded joint, or a monolithic joint will not be pro-

duced at all; this was also confirmed experimentally. When the welding process continues to cessation of free flow, the metal in the welding zone experiences hydrostatic contraction and the rise in the number of dislocations is stopped. The metal having the maximum number of defects is extruded into a flash. As a result of the high mobility of the atoms in the welding zone, the vacant points are filled by atoms which diffuse into the zone of the surfaces that we are butting; the interface between these surfaces disappears. These processes may be studied adequately by metallographic investigation of microsections (at magnifications of 1500-2000) of specimens cut from sections being welded at various stages in welding.

The dislocations and microdefects are seen rather well on microsections subjected to electrolytic polishing and electrolytic etching.

CONCLUSIONS

1. The fundamental possibility of press welding of components composed of aluminum-magnesium alloys at the butt was established.

2. Investigations disclosed the high quality of joints produced by press welding.

3. The method of press-butt-welding aluminum-alloy components with sections to 10,000 mm^2, as developed in the Institute of Electrical Engineering of the Acad. Sci. UkrSSR and introduced to several heavy machinery concerns, can be recommended for broader application.

REFERENCES

1. S.B. Aynbinder, Kholodnaya svarka metallov [Cold Welding of Metals], Izd. AN Latv. SSR [Publishing House of the Latvian SSR Acad. Sci.], Riga, 1957.
2. A.P. Semenov, Skhvatyvaniye metallov [Seizure of Metals], Mashgiz [State Scientific and Technical Publishing House of Literature on Machinery], Moscow, 1958.
3. R.F. Tylecote, Pressure Welding of Light Alloys without Fusion, British Welding Research Association, No. 1, 1946.
4. I.M. Darks, Recrystallization, Welding Journal, No. 5, 1953.
5. N.F. Lashko and S.V. Lashko-Avakyan, Metallovedeniye svarki [Physical Metallurgy of Welding], Mashgiz, Moscow, 1954.
6. R.F. Tylecote, Investigations of Cold-Pressure Welding, British Welding Journal, No. 3, 1954.
7. V. Zayt, Diffuziya v metallakh [Diffusion in Metals], IL [Foreign Literature Publishing House], Moscow, 1958.

Submitted 10 February 1962

DISTRIBUTION LIST

DEPARTMENT OF DEFENSE	Nr. Copies
HEADQUARTERS USAF	
AFCIN-3D2	1
ARL (ARB)	1
OTHER AGENCIES	
CIA	1
NSA	6
DIA	9
AID	2
OTS	2
AEC	2
PWS	1
NASA	1
ARMY	3
NAVY	3
RAND	1
NAFEC	1
SPECTRUM	1

MAJOR AIR COMMANDS	Nr. Copies
AFSC	
SCFDD	1
ASTIA	25
TDBTL	5
TDBDP	5
AFMDC (MDF)	1
ASD (ASYIM)	1